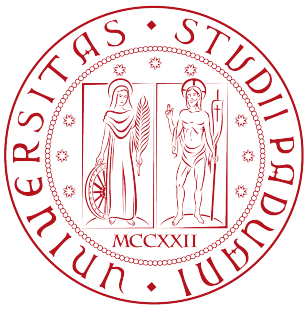

Università degli Studi di Padova

Dipartimento di Ingegneria Industriale

Master Degree in Aerospace Engineering

Integration of a robotic capture mechanism and a quadcopter drone

Author:

Jacopo Cappozzo
2026953

Supervisor:

Prof. Francesco Branz

Academic Year 2022/2023

A papà, mamma, Giorgia, Francesco e a tutte quelle che persone che hanno dedicato una parte del loro tempo per me.

Abstract

The unmanned aerial vehicle (UAV) industry has grown rapidly in recent years. Drones have attracted much attention in recent years due to their ability to be used in hostile environments that are hazardous to humans. They have contributed significantly to avalanche and fire relief, as well as the search for survivors of earthquakes. Due to their increasing use, there has been a trend to build and manufacture drones to carry out planetary exploration. Drone technology has enormous potential to support a number of successful space mission solutions. In the air, some types of activities can be accomplished in less time than traditional timelines over land. Consider transporting scientific samples between two points to appreciate the enormous benefits of solar system discovery. To be used in extraterrestrial environments, UAVs must account for all atmospheric problems such as density, air column movements, chemical composition, temperature, and so on. When referring to Mars, the atmospheric density is approximately 60 times less than that of Earth so the UAVs with much larger wingspans are needed to generate enough lift to fly. The next section of this paper will analyze the advantages and disadvantages of two different planets of growing interest. Mars and Venus are these planets. The objective of this thesis is to test a docking system through a quadcopter in preparation for future extraterrestrial deployments. The drone must be capable of transporting a payload between two predetermined points using a gripper. The quadcopter gripping system was designed through Solidworks and built through a 3D printer. A prototype of the entire system was fabricated and the docking system was tested in a real-world environment. Matlab was used for the post-processing of the sensors fixed in the gripper.

Contents

List of Tables

List of Figures

Acronyms

ABS Acrylonitrile Butadiene Styrene.

BLDC Brushless DC Electric Motor.

CCD Charge-Coupled Device.

CPO Close Proximity Operations.

DoD Depth of Discharge.

EAU Elementary Assembly Units.

ESC Electronic Speed Controller.

GNC Guidance Navigation and Control.

IOA In-Orbiting Assembling.

IOS In-Orbiting Servicing.

PWM Pulse Width Modulation.

TOF Time of Flight.

UAV Unmanned Aerial Vehicle.

1. Introduction

From a technical point of view, unmanned aerial vehicles, commonly known as drones, are autonomous or remotely controlled flying machines. Currently available drones can be of different configurations, can be fixed-wing, rotorcraft and hybrid models; they run on batteries and are capable of carrying payloads and other technical devices that may be needed depending on the use of the drone[5]. The first applications of drones occurred already during the First and Second World Wars where two British programmes: The Larynx and the Ram are mentioned [6]. The Larynx was initially intended to fly a predefined course or "home" on a target while being manually controlled. It was intended to either drop bombs or dive into the target, thereby turning into its bomb, at the end of its 200–500 mile journey. The Ram, in contrast, was more compact and intended to be wirelessly operated from a nearby manned aircraft. Its capacity to "ram" into hostile air formations gave rise to its nickname. By doing so, it might serve as a ruse to draw enemy fire or as a bombing target while manned aircraft stayed at a safe distance.

Drones have attracted a lot of attention in recent years as their use brings improvements not only in the military field but also in industry, research, and public administration. For instance, major logistics firms like Amazon, DHL, or UPS are looking at using drones as a substitute for other forms of transportation[7]. This goal may become feasible as the cost of carbon has come down in recent years, which then translates into lower prices for drones, thanks to improved lithium polymer batteries and also improved obsta-

cle detection and avoidance techniques. In agriculture, drones are used to spray pesticides to avoid humans' health problems when they pour manually [8]. UAVs can be used easily where manpower and equipment are difficult to operate. In industrial environments, they support the safe inspection of inaccessible, hard-to-reach infrastructure, the development of 3D plant models, or the delivery of spare parts[9]. Drones are considered a disruptive technology in the fields of healthcare, emergency services, and disaster management in addition to commercial and industrial uses. Drones have the ability to convey a variety of medical supplies[10] (such as blood samples, AEDs, and COVID-19 test kits)[11], support SAR operations[12], and provide airborne post-disaster damage assessment in this situation[13]. Fire departments, cave rescue teams, emergency medical services (EMS), and even the police are attempting to fast incorporate drones into their operations in order to take advantage of their benefits. Even in the field of mountain rescue, the use of drones sparks interest. Mountain rescue (MR) services investigate drone applications to provide rapid times to respond to emergencies, some examples are the location of the safe path to reach accident sites, the location of avalanche victims, delivery of critical emergency items, and mapping of dangerous and remote locations.

1.1 Space Exploration through UAVs

It can therefore be seen that the use of drones is most significant when dealing with harsh and unhealthy places for humans. Because of this, another field to use UAV is space exploration. The techniques used to explore planets have limited mobility and low resolution and provide limited information about the planet, as a result, it may be interesting to use drones. Exploiting space through UAVs will offer several advantages such as better observation compared to satellites and orbiters used till now. UAVs have the ability to offer real-time services at the network's edge. UAVs can map a sizable portion of the world and collect information from intelligent settings, for example, a sensor on the ground sending data to a wireless gateway server which in turn transmits it to the

drone[14]. Technologies developed for these missions can also bring benefits to everyday life on earth.

1.1.1 Design of UAVs

Since each extraterrestrial environment has different characteristics, the geometry of individual drones must adapt to the planet context and the restrictions imposed by the launcher in terms of size. For planetary exploration, there are several configurations:

- *Balloons and Airships*: airships is a class of aerostat or lighter-than-air aircraft that has its own propulsion system. Airships are distinguished from other types of hot air balloons, hot air balloons and free gas balloons that are subject to the winds (they are immobile in the moving air mass) and are therefore only maneuverable vertically. In fact, the balloons have great difficulty changing trajectory and the energy is used only by the mounted instrumentation. Balloons also struggle to maintain their position. Particular consideration is given to using balloons to explore Venus' surface. This is due to Venus' atmospheric carbon dioxide's notable advantage of enabling a far larger range of balloon-lifting gases (not only the hydrogen or helium that balloons on the ground typically use). In Venus atmosphere, oxygen and nitrogen are used like gas lifters.

- *VTOLs (Vertical Take-Off and Landing)*: it is an aircraft that takes off and lands vertically, without the need for a runway. It is a mix between multi-copters and fixed-wing aircraft, it has the advantages to fly in a high atmosphere and take off without a runway. Propellers are used to generate the thrust and due to this, it cannot reach supersonic speeds. Research on VTOL vehicle efficacy is being done to assist missions to Venus, Titan, and the surface of Mars.

- *Gliders*: it is a heavier-than-air aircraft that sustains itself in flight thanks to the dynamic reaction of the air against wing surfaces and whose free flight does not

depend on an engine. A team from the University of Arizona wants to use a glider in Mars's atmosphere and keep it in the air by exploiting hot updraft columns[15].

- *Flapping wings/Ornithopter*: the idea of building these aircraft came from the flight of birds, bats, and insects. The air density, wing area and velocity affect how much lift a wing produces. Perhaps innovative flying ideas, like flapping wings, can be successfully used in this viscous and low-density environment. The beating of wings requires a lot of power and this is a disadvantage since the more energy is needed, the more the weight has to increase.

Table 1 summarises the various designs used in different applications.

Parameter	**Type of UAV for space exploration**			
Objective	**Airship/Balloon**	**VTOL**	**Glider**	**Flapping Wing**
Data transmission	/	✓	/	/
Massive payload	✓	/	✓	✓
Endurance	✓	limited	✓	limited
Resolution image	✓	✓	✓	limited

Table 1: *Comparative table of several planetary exploration UAV models.*

1.1.2 Mars missions

At the moment, probes and autonomous robots are in charge of planet exploration in order to pave the way for human settlement. All of the inner planets and a few of the outer planets have been reached by automatic exploration systems, but Mars has received the majority of attention in the past two decades[16]. The colonization of the "red planet" is now among the feats of human ingenuity that can be accomplished in a few years and is no longer a science fiction fantasy thanks to the ongoing advancements in aeronautical and electronic technologies. The probes and the multi-wheel rovers that can make straightforward judgments and carry out a variety of tests are the forerunners

of this last stage. Due to the tough Martian soil, their movements are extremely careful. The movements depend on the day-night cycle since there is a high thermal deviation. On the other hand, there are observation satellites in Martian orbit equipped with the HiRISE (High-Resolution Imaging Science Experiment) that is able to map the ground with great precision from 450 km to the surface. It is evident that it is necessary for an hybrid vehicle. It should has the capacity to collect high-resolution pictures and sensor data across sizable regions of the Martian surface. For a long time, robotic aircraft have been suggested as practical resources for Mars exploration[17].

The Environment

Since the beginning of the solar system's exploration, Mars has consistently drawn the most scientific attention from the world community and the various space organizations, as evidenced by the significant investment spent in its research. Although the planet has been studied for centuries, it wasn't until the space era that humans were able to fully comprehend many of its previously only-theorized qualities. It was possible to gather a wide range of data from the composition and internal structure to the interaction of the upper atmosphere with the solar wind thanks to the space probes in orbit and the vehicles on the ground. The Martian atmosphere is rarefied, the highest atmospheric density on Mars is around 0.020 kg/m3, which is equivalent to the density that may be found 35 km (22 mi) above the surface of the Earth[18]. This low density required the use of large-wing area airplanes (low-wing loading) since, as we can see in the ratio below, the lift force is almost three orders of magnitude smaller. The formula of the Lift is:

$$L = 1/2\rho v^2 C_L S \tag{1.1}$$

Where C_L is the Lift coefficient, S is the surface area and v is the velocity. The atmospheric density of the Earth(ρ_E) and the Mars (ρ_M) are:

$$\begin{cases} \rho_E = 1.225 Kg/m^2 \\ \rho_M = 0.0020 Kg/m^2 \end{cases} \tag{1.2}$$

So the ratio of the two lifts is:

$$\frac{L_M}{L_E} = \frac{\rho_M}{\rho_E} = 0.001632 \tag{1.3}$$

Another disadvantage comes from the speed of sound since it is lower than the speed of sound on Earth. This means that you approach transonic speed much faster at the same rotor speed.

$$\frac{v_M^{sound}}{v_E^{sound}} = \frac{240 m/s}{340 m/s} = 0.705 \tag{1.4}$$

The high velocity and the low flight altitude in dim light pose difficulties for imaging systems. Another problem is the Martial temperature since the average temperature at the surface is 63°C below zero, with lows of 140°C below zero and highs of 20 °C above zero (Figure1).

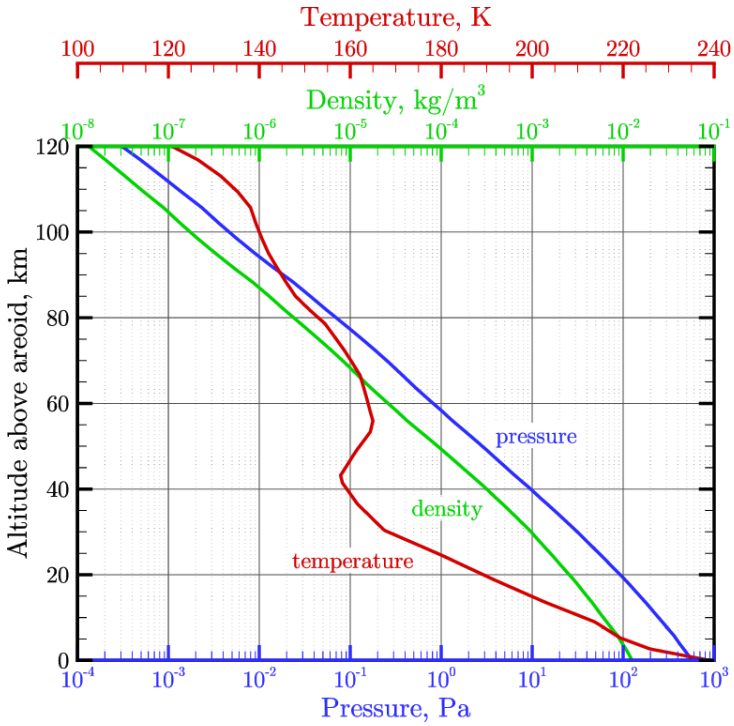

Figure 1: *Mars atmospheric pressure, temperature, and density as functions of the altitude relative to the asteroid[1]*

These low temperatures have a great impact on the avionics, the payload, and the battery. The battery and electronic temperatures in landers and rovers can dip to -60°C at night and increase to 60°C during daytime operations if an excellent thermal management design is not used. Low temperatures may cause batteries to freeze and frequent exposure to extreme temperature changes will wear devices out and cause them to malfunction[19]. In the past passive technique to control the thermal state were used such as high-performance thermal insulation. For the active thermal insulation there were electrical heaters, and radioisotope heater units. This design saved the batteries from low temperatures however, daytime operations were limited to keep internal heat dissipation from causing excessive temperatures. There are some pros due to the atmosphere such as the aerodynamic coefficient of drag being notably lower, so it is possible to build lighter structures.

Mars UAVs

The Mini Sniffer aircraft was the first Mars Uav. It was designed in 1977 and 1978 by NASA Dryden Research Center, Developmental Sciences, Inc., and the Jet Propulsion Laboratory (JPL)[20]. It was one of NASA's initial attempts to create an aircraft with a variable-load propeller that could detect turbulence and monitor both naturally occurring and man-made atmospheric contaminants at altitudes beyond 80,000 feet, but it was never put into flight[21]. The Mini-Sniffer concept made use of the heat generated by a tiny steam engine, which in turn propelled the propeller, which was powered by the reaction of hydrazine with a catalyst. The Mini Sniffer has shown that two challenges faced by Mars aircraft could be overcome: it could fly in thin air and create all of its power using the gasoline onboard. Three Mini Sniffers were built but they had problems with the hydrazine propulsion or with the design of the wings/canard. JPL provided funding and instructed Developmental Sciences, Inc. to carry out a thorough feasibility study on a Mars aircraft. Based mostly on the Mini-Sniffer design and sailplanes, NASA Dryden Research Center, DSI, and the JPL presented many other unmanned aircraft designs for Mars exploration in 1977 and 1978 as a result of the study.

One of the many concepts was the Astroplane from DSI. A fixed-wing aircraft with a hydrazine fuel engine and propellers was the design. The wing area was 20 m^2 (215.3 ft^2) and a mass of 300 kg (661.4 lb). The Astroplane was built with a complicated folding system that included six wing folds, three fuselage folds, and a folding propeller in order to fit inside a 3.8 m (12.46 ft) diameter Viking-like aeroshell. Before the project was abandoned in 1978, a prototype of the concept had been built and some testing had been done. The Astroplane project by DSI contributes to a better understanding of the difficulties of flying on Mars and potential solutions to those difficulties. NASA, businesses, and academic institutions all performed studies in the 1980s and 1990s to look at potential strategies for Mars aviation missions. More sophisticated Mars aircraft designs resulted from significant advancements in technology fields including propulsion ideas, materials, and energy storage. Alongside the technology, a wide range of cutting-edge ideas such as

inflatable wings, solar-powered aircraft, specialized helicopters, lighter-than-air balloons, and flapping insect robots developed.

In 1998, the Mars Airborne Geophysical Explorer (MAGE) was proposed by NASA Ames in association with Malin Space Science Systems, the Naval Research Laboratory, and Orbital Sciences Corporation. The mission objective of the MAGE was to collect data, using a series of scientific instruments, regarding the formation and evolution of a system of canyons and chasms known as the Valles Marineris. The MAGE had a 9.75 m (32.0 ft) wing span, a 135 kg weight, and low-drag flying wings (298 lb). Numerous folds were integrated into the design to allow for storage and eventual deployment of the aircraft from an aeroshell. A 3-bladed propeller located at the back of the aircraft was powered by a hydrazine-fueled engine, as was the case with the 1978 Mini-Sniffer model.

In 1999 NASA publicized the Mars Micromission Project with the goal to discover the Martial atmosphere. NASA Ames, one of the three teams who participated in the feasibility study and conceptual design of the mission, proposed the Canyon Flyer which provides high-resolution imaging of prominent surface features such as the Valles Marineris. The Canyon Flyer was an airplane with a fixed wing, fitted with a 4-blade propeller. Its mass was 14.6 kg (32.2 lb), the wing area was equal to 0.77 m^2(8.29 ft^2), and its estimated endurance and range were 0.25 hours and 130 km (80.8 mi).

The work in [22], presents the design of one of the most interesting Mars Airplanes ARES (Aerial Regional-scale Environmental Survey). The ARES mission was to inspect the structure and the evolution of Mars's atmosphere, interior, and surface. The three main areas of research for the science mission were crustal magnetism, the geology and minerals of the crust underneath, and near-surface atmospheric chemistry. Precision aerial surveying was necessary in order to understand also if there is water close to the surface. When compared to observations made at a height of 100 km, the precision airborne survey would enable the mapping of crustal magnetism at a very high spatial resolution, a spatial improvement of two orders of magnitude (62.1 mi). There were two versions of the ARES airplane. The first version is a combination of the previous experiences and studies in

the martial field which, however, was discarded in Phase 1 of the project. The second version is an upgrade of the first version, it was one of the four contenders' missions for the first Scout launch in 2007 but it was not selected. Its mass was equal to 185 Kg with a wingspan of 6.25 m and it is able to fly until 600 Km.

The newest and maybe most fascinating Mars aircraft design is the Mars Helicopter Ingenuity which was launched on July 30, 2020, from the Cape Canaveral Air Force Station, Florida and it landed on February 18, 2021, at Jezero Crater, Mars. This is part of the mission of the Perseverance rover which carried two segments: the helicopter and the base station (Figure 2).

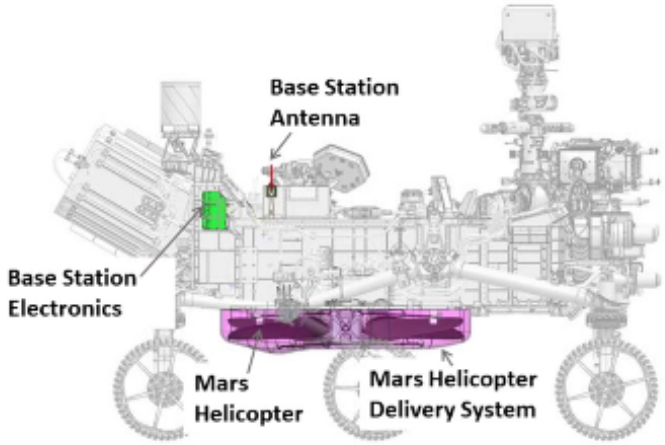

Figure 2: *Perseverance Rover*

The helicopter power is generated from solar panels which charge six Lithium-Ion cells that compose the battery[23]. The battery is under stress at all times because in order to reduce the risk of electrical "brown-out" during any high-power maneuvers performed by the on-board controller, it is necessary to fully charge it before taking off. This aspect limits the amount of time that can be spent on a flight to Mars. During the day the solar panel may then recharge the battery after a prolonged overnight period used to resist the cold. The propulsion system is composed of two counter-rotating rotors having a diameter of 1.21 m, made with carbon fiber and designed to fly in a low Reynolds number regime.

Table 2 shows the differentiation between the parameters of several Mars UAVs dis-

cussed above.

Table 2: *Comparison of the parameters of various Mars UAVs.*

UAV	Power supply	Range [Km]	Endurance [h]	Wingspan [m]	Mass [Kg]
Mini-Sniffer(1975)	Hydrazine fuel	70	1	6.7	75.7
Astroplane(1978)	Hydrazine fuel	10000	17/31	21	300
MAGE(1998)	Hydrazine fuel [24]	1800	3	9.75	135
Canyon Flyer(1999)	Batteries/Hydrazine fuel	130	15 min	2.2	20
ARES(2003)	Li/MnO Batteries	600	1	6.25	185
Ingenuity(2014)	Solar	0.704	1.5 min	1.21	1.8

1.1.3 Venus missions

Venus Environment

Venus is often called Earth's twin because the two planets share a similar dimension, the complexity of the atmosphere and the surface composition. There are significant variances between the two worlds, yet these are not identical twins. Venus rotates very slowly on its axis, completing a rotation in 243.69 days, a period longer than that of revolution. This means that the ground speed required for an airplane to maintain the sub-solar point is extremely low, just 13.4 km/h at the equator. Venus's density is 90 times denser than the Earth's density which generates the greenhouse effect which increases Venus's temperature (more than 470°C on the surface)[25]. Drone designs and concepts that might be employed on Venus have been proposed by researchers and space organizations. Drones equipped with sensors that may capture pertinent data are one method of studying Venus. Even while the climate may be more tolerable at higher altitudes, research vehicles like drones still need to be built with certain considerations regarding thermal system and propulsion system [26]. Indeed, around 60 km from the surface, where the troposphere starts, some of the fastest wind speeds—about 186 m/s—occur. To counter these winds, large amounts of power are required to overcome aerodynamic drag. Energy consumption

tends to scale with weight, so the quantity of energy it takes to fly on Venus also produces an issue to design around. Drones can be more effective exploration vehicles than landers while having more variables to take into consideration. It is simpler to construct for high endurance on Venus because of the atmosphere at greater elevations. Venus has a temperature of around 288 K and a pressure of about 0.2 bar at high altitudes, like 60 km (Figure 3).

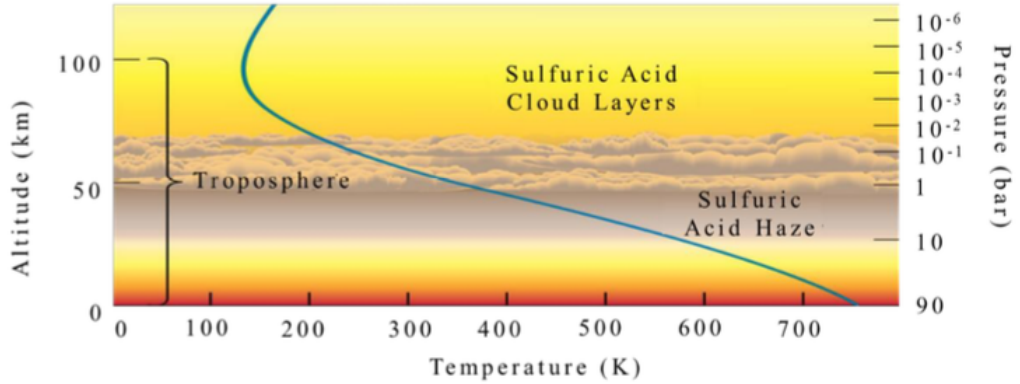

Figure 3: *Structure of Venus's atmosphere*

These circumstances make it easier to design and construct long-term exploration vehicles. Although getting closer to Venus's surface is desirable, exploratory vessels would not survive the harsh conditions. This issue may be resolved with a fixed-wing drone that changes between high and low altitudes. The drone has the ability to fly at lower altitudes to gather information near the ground. The drone will return to higher altitudes where the environment is less severe if it achieves a specific temperature or pressure limit. The drone will be able to cool off during the intersession at this greater altitude.

Venus UAVs

In 2001, Landis suggested that it could be possible to use a solar-powered drone to study Venus's atmosphere. Venus has various benefits for using solar drones since Venus' sun intensity is greater than that of the Earth. He suggested that the design of a Venus drone may be used between an altitude of about 45 km from the surface of Venus, where the

pressure is 2 bars, and an altitude of about 60 km, when the pressure is 0.2 bars[27]. He proposed in 2002 the design of the first solar-powered drone able to fly above the Venus clouds. In order to reduce the cost, the aircraft size must fit inside the aeroshell of the Pioneer-Venus. This aeroshell has some advantages such as:

- the entry vehicle design has already been proven to work in the Venus atmosphere.
- the vehicle dimension is appropriate to launch on a small "Discovery" class launch vehicle.
- small aircraft can be used in mission designs to concurrently deploy a fleet of aircraft, enabling measurements of distinct regions of the atmosphere.

In 2013, Northrop Grumman researchers came up with a proposed Venus Missions called VAMP (Venus Atmospheric Maneuverable Platform) which is an inflatable vehicle used to sample data and observe the surface at 50-70km above the surface. The spacecraft would fly through the upper and middle cloud layers after entering the atmosphere in order to acquire scientific data for transmission to Earth. Due to the vehicle's low ballistic coefficient, atmospheric entry may be done without a bulky aeroshell. As a result, it can support a weight of up to 100 pounds.

In 2015, Xiongfeng et al. proposed a novel sun-seeking eternal flight solar-powered airplane (SESPA) for Venus exploration in altitude ranges from 71.5 to 75 Km. The dimensions are similar to the small drone designed by Landis so the wingspan is equal to 3 m and a chord length of 0.4 m.

In 2016, Husseyin proposed a cycloidal blade system that combined with a stopped rotor system to generate a stopped-rotor cyclocopter drone. The objective of this project is to study Venus's atmospheric composition and the chemical composition of the soil. The innovation in this project is the ability of the cyclocopters rotating blades to be paused and act as a fixed-wing drone.

2. AUTOMA

AUTOMA: AUtonomous Technologies for Orbital servicing and Modular Assembly

As technology advances, more and more emphasis is being placed on autonomous devices capable of performing actions without human intervention. An example would be the autonomous assembly of modular structures that can be homogeneous and thus each module consists of a stand-alone or heterogeneous system, thus more satlets are needed to complete the spacecraft.

This new concept is attracting great interest as it allows satlets to be decommissioned at the end of their useful life by attaching new modules that may concern propulsion, attitude control, and power generation so that they can be moved to orbits of little interest. The use of these missions thus reduces costs and certainly limits the amount of space debris, since it has been a problem for years due to the near saturation of some orbits[28]. Turning to the planetary side, one can see that there is an increasing need for autonomous aerial vehicles for various missions since the methods applied for exploration have limited mobility, low resolution and provide limited information about the planet. UAVs have progressed extremely far in being applied to space missions. The last example is an Ingenuity on Mars which is the first motorized vehicle to fly to another

planet. With the use of these new vehicles, it is now possible to conduct experiments, sensors, or samples more quickly between oneself and a stable base or a rover. These new technologies have revolutionized planetary missions and will make it easier to explore hitherto unknown realities and are therefore a source of investment for many companies. The two applications, despite looking different at first glance, are similar as they use standard technologies in the assembly of modular systems using a dedicated gripper. This innovative project, therefore, deals with the validation of these innovative technologies by leveraging pre-existing studies and technologies developed in the past by researchers.
The main activities will be the validation of an intelligent capture system capable of gripping and managing modules while taking into account all the dynamics of the system through the use of dedicated sensors and nanocomputers.
The smart capture interface will consist of (1) a grasping mechanism and (2) a set of relative navigation sensors and will be designed to be installed either at the end of a robotic manipulator or under a drone. Tests will be conducted within existing laboratory facilities: (1) a robotic structure with a customized manipulator interacting with simulated spacecraft floating on ow-friction tables; (2) a flying arena equipped with motion capture.

State of art

This innovative strategy for using space attempts to lower the cost of satellite development and operation while also taking into account serviceable systems with prolonged operating life thanks to the operations in orbital (IOS). In-Orbit Servicing refers to the capability to perform a range of servicing tasks on existing satellites.
In-Orbit Assembly (IOA) is another operation of the same IOS family and allows additional modules to be attached to existing satellites or structures to be built in orbit. These operations provide a useful alternative for carrying out Active Debris Removal operations since the proliferation of space debris has become one of the principal threats to satellites

and the sustainability of the Critical National space infrastructure. The development of these operations came about through the creation of the international space station (ISS). Humans and robotic systems have to work together to assemble it, by using the ideas of extravehicular activities and human-in-the-loop. These types of works allow us to improve consistently the level of IOS also in the autonomous field, an example can be the Phoenix program by DARPA.

Phoenix seeks to change this paradigm and reduce the cost of space-based systems by developing and demonstrating new satellite assembly architectures and delivery systems in GEO [29]. Phoenix planned to create re-configurable platforms in orbit by combining smaller modules (called satlets) equipped with standard ports for electronics, mass exchange, and data transfer as opposed to depending on big, bulky satellites.

Thanks to this, it will be possible to reduce also the cost of each satellite since it has been shown that the production cost of a satlet can be reduced by increasing its output[30] (Figure 4).

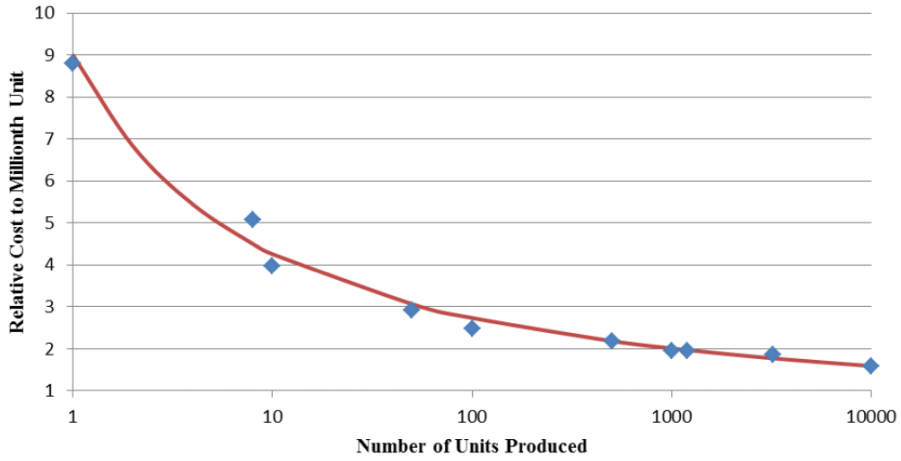

Figure 4: *Normalized Satlet Production Costs*

The Northrop Grumman/Orbital ATK Mission Extension Vehicle (MEV) programme is the cutting-edge in in-orbit servicing and inaugurating the era of reusable orbiters [31]. MEV-I and MEV-II are two successful missions whose goal was to prolong the lives of current GEO satellites whose performances were suffering due to fuel exhaustion. The same

companies are developing successors to MEVs and they will be the Mission Extension Pods, small and less expensive vehicles with which the Mission Robotic Vehicle attaches itself to the dead satellite. Unlike MEVs, which can help to correct already degraded orbits, MEPs will only act to maintain the required course corrections.

MEVs are able to dock autonomously while MEPs require help from a space robot equipped with robotic arms that capture a floating capsule, drive it to the desired target and install it.

NASA's On-Orbit Servicing, Assembly, and Manufacturing (OSAM-1) mission not only aims to dock a working satellite and refuel it to increase its operational life but also to work on its assembly and manufacturing in space[32].

The mission is targeting Landsat-7 a satellite from 1999. The big hurdle will be to autonomously recognize the various worn-out parts of the satellite so that it can be refueled even though it was not designed to take advantage of this exercise.

Other projects can be mentioned in this field like the Deutsche Orbitale Servicing Mission (DEOS) which was a two-satellite demonstration mission on the European side that called for a servicer satellite to carry out a number of tasks on a client vehicle, Caesar, a robotic arm being developed by the DLR for space activities including assembly and service. In the field of exploration planetary, the first test is Ingenuity on Mars which is a small autonomous drone[33]. Its purpose was to prove powered flight in the thin atmosphere of Mars since the atmosphere of the planet is just 1% thick so generating lift is a problem. It is composed of Solar-powered and recharges on its own, it has a wireless communication system, Counter-rotating blades that spin at about 2,400 rpm, and it is equipped with a computer, two cameras, and navigation sensors.

Description

This concept envisions two application scenarios in the sphere of space technology and exploration based on the autonomous assembly of modular devices. The first use is tied

to existing satellite IOS and ADR mission designs, whereas the second provides novel techniques for extraterrestrial planet exploration or distant Earth monitoring.

In the first instance, the mission concept envisions the ability to connect one or more service modules to the target system in order to enhance current satellites, reactivate deactivated platforms, or remove debris. To enable the docking of the servicing module onto the receiving satellite, a chaser vehicle reaches rendezvous with the target satellite and executes the necessary CPOs. The chaser vehicle has a robotic arm and is loaded with a number of maintenance modules known as Elementary Assembly Units (EAUs). EAUs are standardized modules that facilitate the operations of the mechanical arm by having the same interfaces (mechanical, telecommunication and optical). Thanks to these standardized modules, the robotic arm is able to autonomously grasp the EAUs from the magazine and securely attach them to the target.

Depending on the bodies involved, the interface to be used is chosen; if both are optimized, a standardized interface system can be used, otherwise, clamps or adhesive systems can be used to ensure a rigid assembly. In the second mission architecture, more autonomous vehicles and platforms will cooperate to explore Mars without any equipment. The many agents communicate with one another and with the base systems by exchanging information, data, and materials. The fixed bases provide logistical support for aircraft and host scientific experiments or miniature laboratories, acting as independent scientific assessments. Vehicles of many types, like rovers and drones, are used to explore and monitor a large portion of the planet's surface while also providing connectivity and transportation capabilities between fixed bases. This scenario exhibits a variety of levels of modularity. Every machine or base will function, on the one hand, as a node in a modular network that maximizes resource and information sharing.

On the other hand, every agent is designed to be modular in some way, allowing for advanced functionalities like the replacement of components (for instance, the batteries in airplanes) or the expansion of capacities (for instance, the addition of communication or data archiving modules to stationary labs). Adopting UEE as the basic unit of drone

protection enables the execution of a number of advanced operations, such as the replacement of parts at ground bases or the transportation of probes between research outposts and launch bases. The modified drones, equipped with a standard acquisition interface, are used to detect, transport, and assemble EAU onto other agents in the exploration network. In this project, the drone will be remotely controlled and will then execute a predetermined route. the purpose is therefore to validate UAE drone interface to then enable the advancement of this technology toward broader scenarios such as the fully autonomous system. This new paradigm for exploration applies to terrestrial landscapes as well, especially in remote areas with extreme environmental conditions (such as deserts, forests, or hazardous areas) (e.g. response to natural disasters). Application areas include disaster relief, scientific observation, research, and asset recovery.

These two seemingly unrelated domains of application share several technologies whose advancement is essential to their continued existence. Relevant technologies include related docking/capture methods, control and guiding algorithms, and navigation systems. The research team's members have extensive backgrounds in GNC and mechanism technologies, and this project intends to use their collective knowledge to produce a laboratory validation of the key technologies involved in the scenarios presented. The experimental efforts will be focused on demonstrating the viability of close-range relative navigation sensors and intelligent grasping instruments for the capture of semi-cooperative objects. Both of the above-mentioned idea scenarios will be compatible with the created technology.

Characterization and functional verification testing will focus on two key components: (1) a set of relative navigation sensors used for inspecting and estimating the posture of the target item; and (2) a smart gripper mechanism to be mounted on robotic arms and drones. These innovations will be combined into a Guidance Navigation and Control (GNC) system that includes the estimate and control algorithms necessary to complete the loop and make the system autonomous. The research team's extensive knowledge of CPO-related technologies will be crucial to this effort. New technological solutions will

be created, they will be integrated with current technologies, and experimental setups for their assessment will be designed. Through their evaluation within the context of potential application situations, the team's previous solutions will mature in order to reach the desired results.

Definition of experimental scenario

Since it is an innovation, a large part of this project deals with the experimental validation of the technology. The design of test setups and procedures is critical because it is necessary to simulate zero gravity in the first case. This setup choice also will be conducted during the first part of the project. This section reports the first iteration of this task, with a preliminary description of the experiments that will be implemented and carried out. Three main experiments are conceived (A, B, C). The focus will be on the third scenario which is the one that characterizes this paper.

A Scenario A is the Relative motion estimation and control of cooperative/non-cooperative smallsat mock-up on a flat table.

The test intends to validate several relative navigation sensor systems in support of missions like as in-orbit servicing and close proximity operations. The chosen sensor solutions will be drawn from a set of potential possibilities with a range of development phases within the research team. The characteristics of the target object vary for each of the alternative solutions, which are all based on monocular or stereo cameras:

(a) Semi-cooperative target equipped with either passive B/W high-contrast fiducial markers, retroreflectors or code-based markers.

(b) Non-cooperative target; peculiar geometric features of the target as exploited for pose estimation.

The experiment is conducted on a flat table with two modules, a passive target and

a controlled chaser that approaches the target following a given trajectory.

B Scenario B is the Robotic assembly of cooperative nanosatellite modules on a flat table.

The test goal is the assembly of a standardized, CubeSat-sized module (EAU) onto a controlled nanosatellite mock-up floating on a low-friction table. The assembly is performed by an anthropomorphic robotic arm equipped with a smart gripper with integrated sensing and control functions. The manipulator grasps the EAU and puts it in contact with the nanosatellite allowing the docking between them. The robot end-effector features three independent actuators and a suite of Ultra-Close Proximity (UCP) navigation sensors. The final execution of the final trajectory is enabled by the joint operation of the UCP sensors and other navigation sensors. Several options for the semi-cooperative target interface will be considered, including RGB LEDs, retroreflectors or code-based markers. The facility exploited needs to be completed with a 4-camera motion capture system whose procurement is partially funded by this project.

C Scenario C, which concerns the thesis, is the assembly of ground structures with aerial vehicles. The purpose of the project is to demonstrate the feasibility of using drones to automatically assemble and reconfigure small ground structures. Specifically, a UAE is grabbed by a quadcopter drone in this case and assembled into a fixed structure. In this project, only the first part of the complete design is going to be tested. The docking between the end-effector robot and the UAE will then be tested. The standardized payload will then be moved to a predetermined area and not attached to a structure. Therefore, the orientation with which the payload is undocked is not important. The end-effector robot used in test B is analogous to the drone-mounted capture device therefore equipped with three actuators that will contact the payload to be grabbed. The construction of the navigation sensor is the same as in test B. In fact, between UAE and gripper is present, the

phenomenon of led and photo-diode allows approach and centering in docking. In addition, other navigation sensors have been installed to improve the docking which will be explained in more detail in later chapters.

Project objectives

The MAIN OBJECTIVE of this project is to evaluate a set of technologies that enable the autonomous construction of modular structures and that are suitable for planetary exploration and on-orbit servicing and assembly situations. There are two main technologies in the Automa project. These technologies are intelligent capture device that enables autonomous manipulation of assembly modules and a set of relative navigation sensors that provide accurate position estimates between interacting entities. Validation is carried out through a series of planned tests that will provide a thorough understanding of the system's behavior, enabling further improvements and setting the course for future progress. Investigations are conducted in a laboratory environment that simulates real-world environmental circumstances. By encouraging the ideas of modularity, reconfigurability, and operational flexibility in the design of space systems and mission scenarios, this technical objective contributes to the achievement of the GENERAL GOAL. One of the applications that will be used in the future is the automatic construction of structures in space and on Earth (Marte or dangerous conditions on Earth) using a combination of autonomous vehicles (micro and nano satellites, drones), complex robotic multicorporate systems, and other technologies. The thesis focuses on this objective. The main purpose is to point towards the autonomous displacement of standard payloads through drones. Through the two above mentioned technologies allow the realization of this wider objective. The docking system and the set of sensors that allow the approach of the components have already been designed and tested in scenario B. The project's INNOVATION content has a dual nature that reflects the two objectives listed above. Long-term prospects indicate that this research's findings will bring advanced planet-exploration strategies and highly

novel applications related to IOS/IOA paradigms one step closer to reality. The commercial space services sector will change drastically as a result of the ability to do routine maintenance on valuable orbital resources, allowing fewer satellites to be inactive.

The ability to obtain total situational awareness of the surrounding environment and, indirectly, the colonization of extraterrestrial worlds will be made possible by demonstrating the viability of implementing modular networks of autonomous agents in a planetary exploration scenario. A deeper look at the technical specifications shows that the integrated smart design for the capture interface that has been proposed is innovative on its own and will be one of the major technologies that will enable the prospective mission scenarios described. Although being a crucial part of a robotic system, the end-effector is usually ignored during design. The smart device validated in this project implements several innovative concepts like (1) autonomous actuation of each mobile part (fingers), (2) integrated use of different local sensors to support the capture operations, and (3) decentralized (local) computational capability. The following RESULTS will contribute to the fulfillment of the main objective of the activity.

3. Drone

This thesis concerns scenario C of the AUTOMA project described above. In this scenario, the final aim is to test the validity of the gripper mounted on a drone in order to move standard elements to predefined locations. This chapter describes the design and construction of the drone which is what will be exposed in this chapter. For the purposes of this project, the drone had to fulfill specific requirements:

- TO be as lightweight as possible, less than 2 kg since the load remaining to reach the maximum take-off weight can be used for the payload.
- To be sturdy enough to install a gripper on it without having attitude control problems in the flight phase.

3.1 Drone selection

The first thing to do is to select the type of drone. There are two major families of air vehicles: rotary-wing aircraft and fixed-wing aircraft. The main advantages of rotary-wing aircraft are their ability to hover in the air (hovering, or fixed-point flight) and to move in a perfectly vertical manner (vertical flight)[34]. The latter feature greatly facilitates take-offs and landings, particularly when space is restricted or obstacles are present. Rotating-wing aircraft, on the other hand, have slower top speeds and shorter ranges than fixed-wing aircraft. Thanks to their vertical take-off and their ability to stay in the air, the

model chosen for the project falls within the rotary-wing vehicles. The helicopter is the most well-known. It features one horizontal rotor for lifting and moving horizontally and one vertical tail rotor to balance off the main rotor's torque. The main rotor's pitch may be dynamically changed, which allows the helicopter to go forward, backward, or sideways. Dynamic pitch rotors are more complex than fixed pitch rotors. These issues make controlling a helicopter more challenging. Consequently, it is not believed that a helicopter would be the most appropriate vehicle for this purpose. Bicopter, quadcopter, hexacopter, and octocopter are other varieties of rotary-wing aircraft that are available. These aircraft, thanks to an even number of rotors, do not require additional rotors for stabilization as the torques cancel each other out as shown in Figure 5.

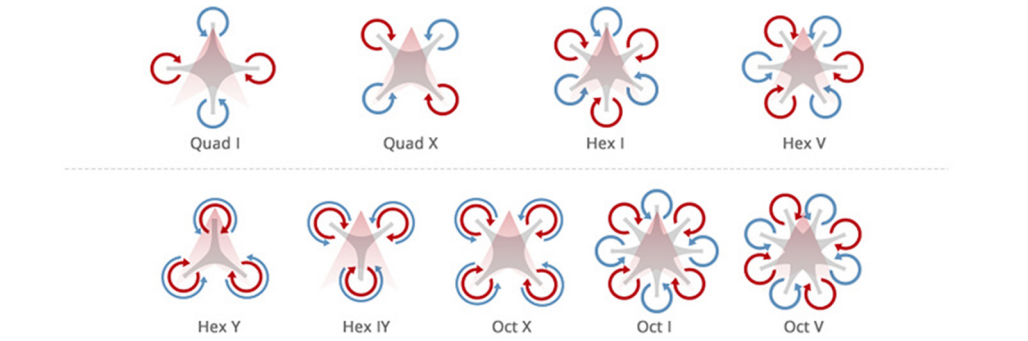

Figure 5: *Types of rotary-wing aircraft depending on rotor arrangement.*

For the same type of engine, the greater the number of motors, the greater the load capacity and the flight safety of the drone. A hexacopter having 6 motors 120° apart, if one of its motors is damaged or stops working, the remaining 5 take over (additional redundancy). This means that a pilot will be able to land safely even when one motor is damaged. For a normal 4-propeller drone, this would be much more difficult, if not impossible, to do. A larger number of rotors allows the position to be varied more precisely, tilting the drone by a smaller angle as the motors are closer together, so instead of imparting a large thrust on a single rotor, a small thrust is applied to several motors. It was decided to use an X-quadcopter for this application since it possesses a neutral configuration between tricopters and hexacopters in terms of complexity and weight. A

quadcopter's basic structure comprises four rotor assemblies that are connected to a central hub via four arms. Every rotor is in a single plane and produces thrust perpendicular to the drone. The plate for the rotors are fixed, unlike in bicopters that require a moveable platform for both its rotors to achieve stability and forward motion. The geometry of the UAV is symmetrical. Given a certain input, each rotor must be able to generate an equal amount of thrust in terms of torque. So since each rotor generates a force during rotation as a result it generates an opposite force, according to the principle of the third law of dynamics [2]. If the propeller has a clockwise revolution, the motor that sets it in rotation will tend to rotate in the opposite direction, that is, counterclockwise. This creates a serious problem of directional stability since the rotors are mounted in a horizontal plane and the reaction torque is unloaded on the machine frame on which they are fixed. In fact, if all four rotors were to rotate in the same direction, the drone frame would spin vortically in the opposite direction without any possibility of control. To overcome this drawback an opposing torque must be generated by having half of the rotors mounted on the machine have an opposite revolution so as to cancel the reaction torque produced by the other half of them. To give an example, on a four-rotor multirotor two of them will have a clockwise revolution (CW) while the other two will have a counterclockwise revolution (CCW). This mechanism will generate reaction torques on all four rotors, but they will cancel each other out. This is a benefit of the quadcopter design as it eliminates the requirement for extra gyroscopes or rotors on the vehicle for the express purpose of reducing undesired torques on the aircraft. To move horizontally, an X-quadcopter has two rotors inclined down and two tilted up (see Figure 7). Brushless DC Electric Motor motors are adopted to drive the rotors. BLDC motors are more efficient than brushed DC motors and are controlled by a Pulse Width Modulation signal, allowing for very accurate digital speed control.

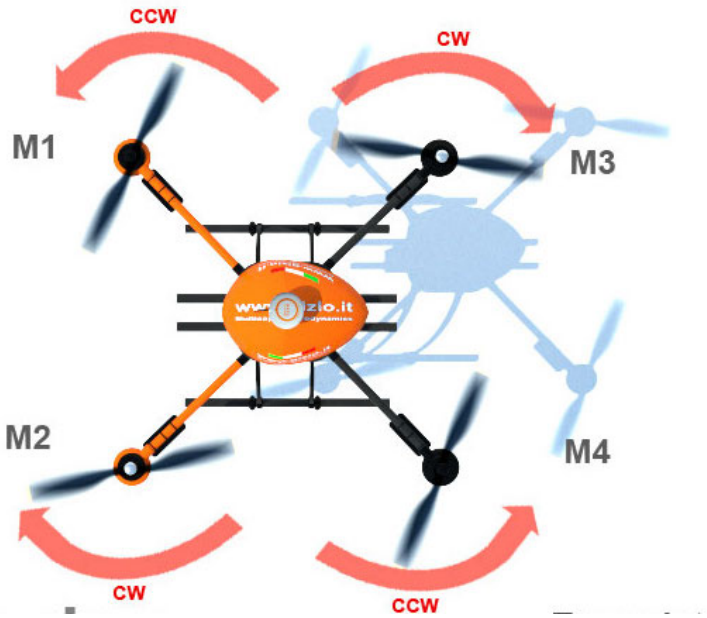

Figure 6: *Torque generated by the motors[2].*

Figure 7: *Horizontal movement of a quadcopter.*

3.2 Components selection

The main parts of the drone are:

1. Frame
2. PX4-Flight computer
3. Brushless motors with ESC
4. Propellers
5. Battery
6. Radio System

Frame

The Frame of the drone is a DJI f450. It is composed of a carbon central body which is located at the center of mass and four plastic arms providing connections for the motors. The shape is not designed aerodynamically because the drone does not need a control surface. The frame weight is equal to 282g. Geometry dimensions are shown in Figure 8. To enable the installation of the gripper, landing feet were mounted so that the gripper would not touch the ground in the first place.

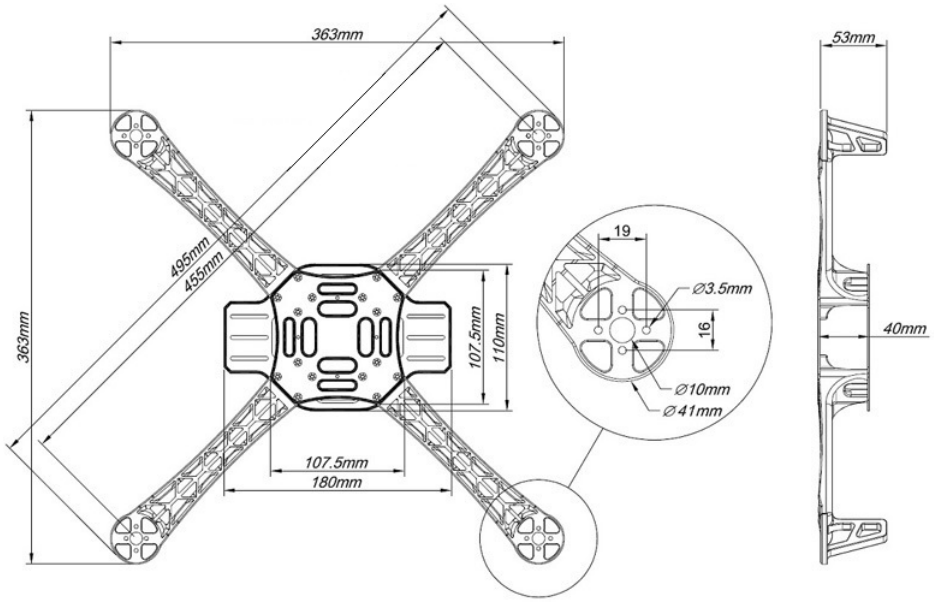

Figure 8: *DJI f450 frame.*

PX4

The most important part of the drone is the mRo Pixhawk 2.4.6 autopilot (PX4). It is a well-known general-purpose flight controller [35] (see Figure 9).

Figure 9: *PX4 flight controller.*

The behavior of the vehicle while performing various maneuvers is controlled by the flight controller, which collects input from sensors and conducts computations defined in the control strategy. PX4 provide with 4 sensors:

- ST Micro L3GD20H 16 bit gyroscope
- ST Micro LSM303D 14 bit accelerometer/magnetometer
- Invensense MPU 6000 3-axis accelerometer/gyroscope
- MEAS MS5611 barometer

These sensors compose the IMU (Inertial Measurement Unit) that is needed in every drone for the stability. It must respond instantly to all outside disturbances in order to stabilize the drone. The UAV generates a rotational acceleration when an external force is applied, and the gyroscope detects this acceleration. The flight controller instructs the motors to apply an equal rotational acceleration in the opposite direction based on the direction and strength of the rotational acceleration. The impact of an outside disturbance is reduced in this way. The current position of the drone and its trajectory to the target can be calculated using IMU acceleration data through the dead reckoning method. Dead reckoning is a simpler navigation technique that is based on route estimation from antecedent parameters. Although the quadcopter has a GPS module for location and navigation, when the GPS is not working, dead reckoning is employed. For this project,

a 3DR GPS is used to obtain better results and better stabilization. Thanks to gps navigation, the drone is able to stay in hover at a given point so the more satellites are in view, the higher the position accuracy. Uncertainty about position accuracy allows for a more or less stable hovering drone.

Brushless

A brushless DC motor is an electric engine powered by a direct voltage supply and that does not require a brushed commutator like the traditional electric motors. For the purpose of this paper, four sets of brushless DJI 2212-920KV were used (Figure 10). These motors have been because they have a thrust of 6 N as can be seen from Table 3, which thus allows a margin of safety in the total weight of the assembly.

KV	920	rpm/V
Max Power	370	W
Max Thrust	620	g
Weight	53	g
Shaft Diameter	4	mm

Table 3: *Motor technical characteristics.*

Figure 10: *sets of brushless DJI 2212-920KV.*

A DJI Esc E300 [36] was used to calibrate the current required by the motors. These

ESC are OPTO (Table 4). OPTO stands for "optocoupler," a way to electrically isolate the ESC from other electronic parts. That's an LED sending a light signal across a small gap to a photo cell that receives it, so no electrical connection between the two sides. This can be advantageous when dealing with very high voltages and/or currents, since the voltage ripple generated in the power supply by the motors themselves can be quite high, especially during high-revving acceleration or braking, and can return to the control electronics through the ESC's power or control cables. However, even some quadcopter ESCs are known to have optocoupling. Since the purpose of optocoupling is to not have the Flight controller (FC) electrically connected to the ESC, it is almost completely excluded from having a battery eliminator circuit (BEC) built into the ESC. These ESC are less affected by the electromagnetic effect of the components thus allowing the sensors to operate more accurately.

Current	15	A OPTO
Signal Frequency	30/450	Hz
Voltage	11,1/14,8	V

Table 4: *ESC technical characteristics.*

Propellers

The number of propellers, their diameter and the pitch of them are all elements which are used for a classification. Increased thrust is created by propellers with more blades, and the vibration is decreased. The quadcopter prototype uses plastic propellers that are easily available on the market. The propellers used have a diameter of 238,76 mm, a pitch of 109,22 mm and a weight is 13 g. The drone's primary function is determined by the propeller's pitch. High pitches are used for a racing drone to avoid loss of thrust during acceleration and maneuvering. Smaller pitches, on the other hand, are to be associated with propellers with larger diameters since they allow to lift bulkier and heavier models while maintaining a relatively high range. For this project, a balance between the two

fronts has been. These DJI propellers have the special feature of being self-locking and therefore do not require an additional system to hold them. Propellers lock based on the rotation of the motor, so there are two types: one that screws clockwise and one that screws counterclockwise.

Battery

The prototype's motors need 12 DC volts to work. BLDC motors use a lot of current. A 15A ESC is needed, per the requirements, to run a single 920kv BLDC motor. Since there are four motors in total, the maximum current consumption for the motors operating at full speed is 60A. This is the reason why a battery with a high DoD is used. As a result, a LiPo (Lithium-Polymer) battery with 4 cells was used for the prototype, where each cell has a voltage equal to 3,7 V for a total of 14,8 V. The capacity of the battery pack is 2600 mAh. LiPo batteries are common batteries for drones because they have a high discharge rate and are lightweight. The flight computer and other components require much less current compared to motors, about 2 A.

Radio System

The chosen radio system of Futaba was chosen according to the possibility of using 2.4 GHz FHSS radio communication with an almost complete absence of interference, unlike in FM broadcast systems. In this type of transmission in fact the bandwidth of the signal to be transmitted is considerably lower than that of the band in which it is possible to transmit, and therefore the transmission channel within the transmission band is varied randomly in order to be less sensitive to interference. The system, consisting of 8 different channels[3], consists of a Futaba R2008SB receiver and a Futaba T8J control radio.

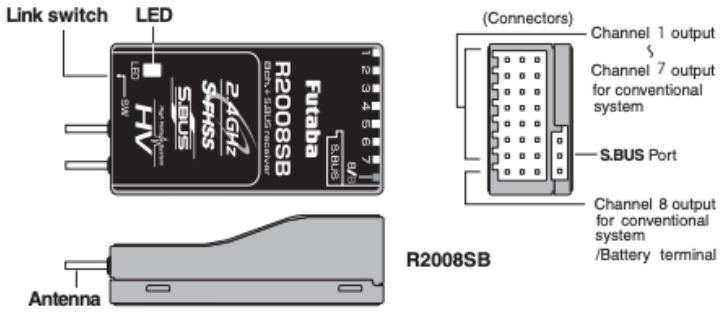

Figure 11: *Futaba R2008SB receiver[3]*

3.3 Power budgeting analysis

One of the first steps was to validate the actual feasibility of the design, although a priori the weights and consumption of all the various elements were not known exactly but could only be estimated through data sheets. Using the software Ecalc [37], it is possible to choose from pre-installed libraries the components that make up the drone in order to obtain the final configuration. The range of the drone was then checked by assuming a weight of 1200g. The total weight is the rounded-up sum of 280g battery, 60g propellers, 42g raspberry, 282g frame, 212g motors, 20g ESC, 15g Px4, 165g first version of the gripper and around 50g for the cables. A safety factor was considered in the calculation since some items such as cables have been estimated with some approximation. The software results are shown in the tables below (Table 5 and Table 6) and in Figure 12. The highest endurance is found with the drone in hovering in fact reaches 15 minutes of flight time while with a mixed flight the flight time drops to 9 minutes. Since the main objective is to test the interface between the gripper and the payload, the time of flight around 10 minutes is sufficient to allow this event. With the motors at maximum, the required current is 19,07 A. The chosen ESC's deliver a maximum of 15 A to the motors, so the rotors will never be pushed to full power. This data is not relevant to the project since the power output at optimal regime is already sufficient to complete the various tests.

The max thrust (6 N for each motor) allows the payload to be safely lifted and ensures

	Battery	
Load	28,32	C
Voltage	13	V
Nominal Voltage	14,8	V
Energy	39,96	Wh
Total capacity	2600	mAh
Utility capacity	2395	mAh
Mixed flying time	9	min
Hovering flight time	15	min

Table 5: *Battery test.*

Motor	Optimal efficiency	
Current	10,87	A
Voltage	13,66	V
Speed	11507	rpm
Electric power	148,6	W
Mechanical power	127,4	W
Efficiency	83,9	%
Max thrust	6	N

Table 6: *Engine testing under optimal conditions.*

Motor	Maximum	
Current	19,07	A
Voltage	12,8	V
Speed	9914	rpm
Electric power	244,1	W
Mechanical power	196,9	W
Efficiency	80	%

Table 7: *Engine testing under maximum conditions.*

an adequate safety margin for the final weight of the drone. Figure 12 evaluates the range and flight time in the two different possible configurations, the ideal frictionless one and the one with an average air friction value. The curves regarding mean friction are visibly lowered compared to the ideal ones but reach values in line with what is desired. This gap is created by the resistance created by air friction on the body of the drone but especially on the propellers.

3.4 Software

Ardupilot is the code used in this project to program the flight computer on the drone. It has been since it is an open-source autopilot system supporting many vehicle types: multi-copters, helicopters, fixed wing aircraft, boats, submarines, rovers and more [38]. This code first of all is compatible with the flight computer and the other installed hardware. To run the code it is necessary a GCS (Ground Control Station) which is often a software application that connects to the UAV by wireless telemetry and runs on a computer on

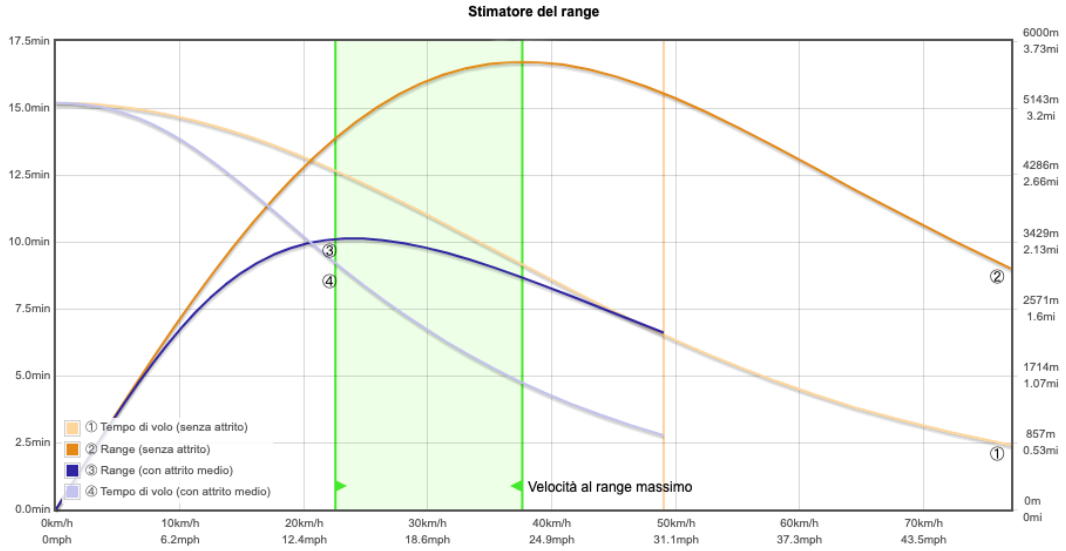

Figure 12: *Drone range and flying time.*

the ground. For this project, the host to run the code is Mission Planner. The major goal of the software is to offer the pilot control of the vehicle, either automatically or with input from a companion computer on board, a ground control station, or a radio control transmitter. Any of these methods are optional, depending on the need and objective you choose the best configuration to control the drone. After connecting all components to the on-board computer, the drone was connected to the PC via a USB to allow the firmware to be installed chosen according to the mounted FC model. The last step to complete the drone is performing initial configuration and calibration. This step is divided into several parts which are :

- Frame Type Configuration.
- Motor Numbering and Direction: the motors should be numbered so as to impart to them the exact rotation to eliminate the torque present.
- Radio Control Calibration: RC transmitters enable the pilot to control the vehicle's movement and orientation as well as the flight mode and to switch on/off auxiliary functions (i.e. opening and closing a gripper, etc). In order for ArduPilot to properly understand the input, RC calibration essentially takes the minimum, maximum, and

"trim" values for each RC input channel. Each channel was then labeled to a main flight command: Roll stick should control channel 1, Pitch stick should control channel 2, Throttle stick should control channel 3, and Yaw stick should control channel 4.

- Accelerometer Calibration: The autopilot's accelerometers must be calibrated to compensate for any off-axis fluctuations as well as their bias offsets in all three axes. Calibration was performed by rotating the drone along each axis. The software permits a second calibration (Calibration Level) before the flight, which can only correct differences in pitch and roll but not yaw, and which can correct a maximum of 10 degrees of the difference between the initial calibration and the final position in the vehicle.

- Compass Calibration: Compass calibration must be done with a good GPS signal so as to ensure the best setup. The vehicle must be kept in the air while being rotated so that each side shows the ground for a brief period of time each. Six complete turns will be made if you consider a full 360-degree turn with each turn directing the vehicle in a different direction toward the earth.

- RC Transmitter Mode Setup and Flight Modes: Three flight modes were supported (using a three-position switch) by configuring the transmitter to produce PWM pulses of 1165 ms, 1425 ms, and 1815 ms for the respective switch positions. The flight modes are: Stable, Auto and Manual.

- ESC Calibration: This section is not necessary since DJI chosen ESCs are already calibrated.

Once the last step is completed, the network of connections between the various elements in addition to the drone such as the radio control can be defined. As it can be seen in the block diagram below (Figure 13), the data exchange between drone and computer is done through Mavlink. It is a protocol for communicating with small unmanned vehicles.

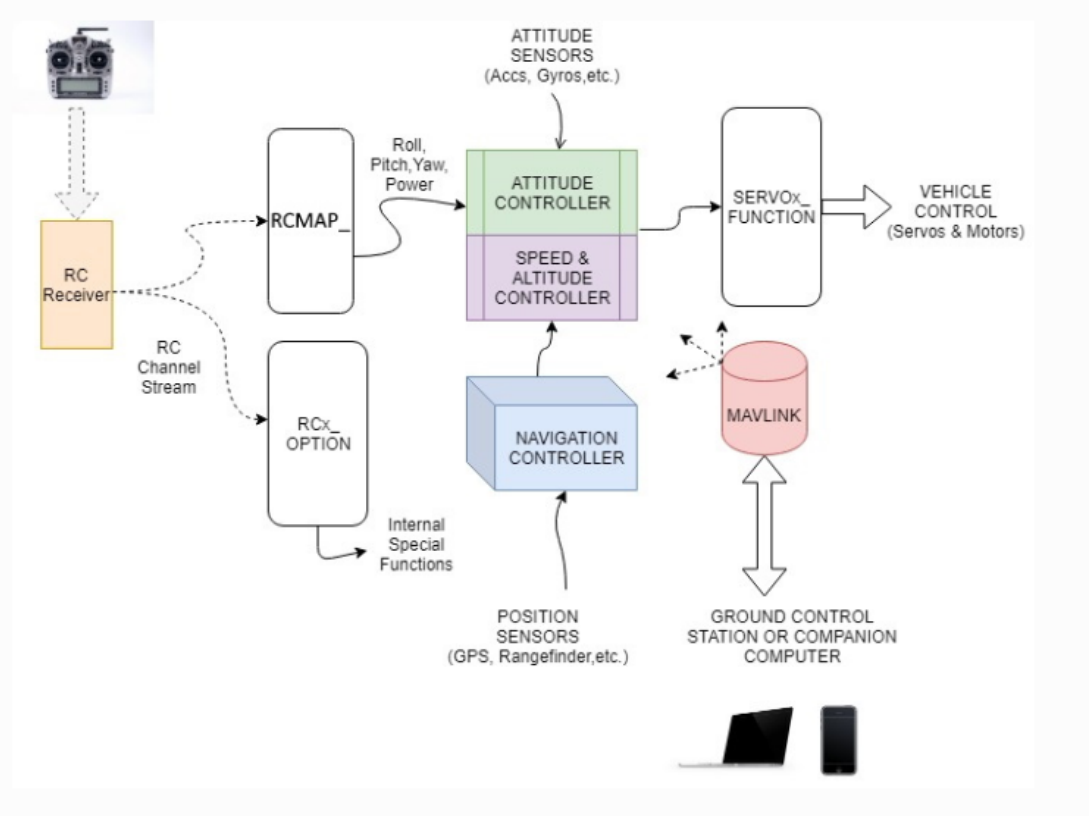

Figure 13: *Simple block diagram of the drone input/output[4]*

Two types of signals come out from the transmitter: RCmap which is essential for piloting the drone and the RCx Option which is used to control the three gripper servos. These transmitter signals are the inputs to the FC, which, thanks to the internal IMU, processes the data and sends appropriate corrections to the servos. The Autopilot makes sure to adjust the motors individually in such a way as to control the intensity of the various torques that are generated, such that they cancel numerous times per second of flight. Through the processing of special algorithms, the Autopilot acts on the ESCs in such a way that these units constantly vary the rpm of the motors with the aim of balancing the mutual torques.

4. Gripping system

This chapter provides an extensive description of the Gripper attached in the lowest plane of the drone. The capture system should be a standalone system. The design and gripping systems must be able to function without depending on the drone. In this fashion, the drone only serves as a positioning system for the capture tool, while the tool can estimate the target's pose, implement the necessary algorithms and logics, make a decision, and then catch the payload with the dedicated actuators. As a result, the gripper can be used with any type of drone without having to check the underlying architecture. The target interface has the same challenge. It must be passive and acts just as a grappling feature in order to establish the connection between the drone and the payload. The main parts of the gripping system are:

- A grasping device, such as a gripper with a symmetric design described in Paragraph 4.1.

- A group of sensors that allows an approach to the target. The first sensor is a matrix of phototransistors and a second is a group of three Time-Of-Flight sensors. These sensors are only used to measure vertical and horizontal distances. The problem of rotation is not considered since the gripper and target are symmetrical (see Paragraph 4.2).

- A computer (Raspberry Pi model 3B+), to allow the gripper to approach and

capture the payload (see Paragraph 4.3).

- A payload whose design was delineated considering the placement of certain sensors and elements necessary for docking (see Paragraph 4.4).

4.1 Gripper design

The initial design of the gripper is the result of a project predating this thesis[39]. The initial gripper served as an end effector of a robotic arm for an orbiting satellite. Since the scenario of interest has changed, it is necessary to adapt the gripper design to it. Therefore, two different versions were studied in order to install it under the drone. The difference between the two versions lies mainly in the mechanical finger actuation system: linear actuators were adopted in the first version, while rotary servo motors were adopted in the second version. The material used for all the pieces designed in this session is ABS, and the manufacturing process is done using 3D printing. Acrylonitrile-butadiene-styrene is a common thermoplastic polymer used to create lightweight, rigid objects with an operating range of -20° to 80 °C. One of the common parts between the two versions is the plate to mount the gripper to the underside of the drone. The plate was designed by using Solidworks (Figure 15). The shape of the plate is designed to be in contact with the base of the drone while avoiding the obstructions created by the support feet.

The three holes in the center are for connecting the standoffs of the gripper while those ones above are for connecting with the drone. The bracket has a symmetrical design in order to distribute homogenously the active forces.

Once the plate was optimally designed, the next step was to define out the most convenient way to attach it to the drone. Two different types of plates were designed for this fixing system: Plate A and Plate B. Plate A is used to increase the contact surface area on the overlying plate so that there are no points overstressed by the weight above. Plate B, on the other hand, is designed to prevent rotation between the bracket and the drone's lower base. Their thickness is therefore the same as that of the drone base so

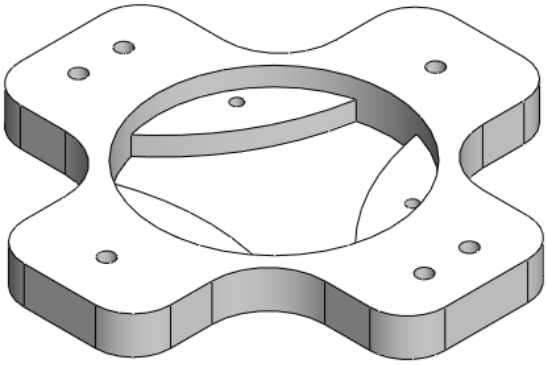

Figure 14: *Bracket designed for drone gripper connection.*

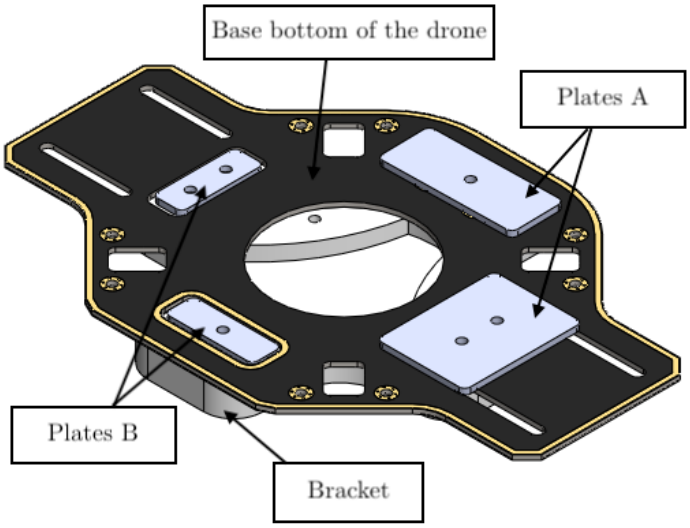

Figure 15: *Bracket attachment system to the drone.*

that plate A can be fully supported against that of the drone. These plates are held in place by screws with M3 thread. The second common element between the versions are Standoffs. Standoffs were used for the connection under the plate between the bracket and the central body of the gripper. The standoff is 4 cm in length and has an M3 threading. They were chosen because they have small cross sections since they are made of steel. By doing so, space is gained to allow the electrical cables to pass through since the gripper sensors require a flat cable with 50 wires, two for each phototransistor. The fundamental part of the system i.e. the Gripper is composed of three fingers independently actuated spaced 120 degrees apart. Both versions use the same central body. The central body was modified from the existing one by removing the parts where there were sensor housings

Gearing Option	100:1
Peak Power Point	40N @ 6mm/s
Max Speed (no load)	10mm/s
Max Force (lifted)	50N
Max Side Load	10N
Back Drive Force	35N
Stroke	20 mm
Input Voltage	6 VDC
Stall Current	550mA @ 6V
Mass	21g

Table 8: *PQ12 Specifications.*

not used in this project. The body was then shaped to decrease the total weight while maintaining the necessary strength for the gripper and it is drilled internally to place the sensors required for docking.

First Version

The first version of the gripper used a three PQ12 100 R Miniature Linear Motion by Actuonix as the power mechanism. The PQ12 actuators are fully integrated, independent linear motion systems with position feedback for complex position control capabilities or end-of-stroke limit switches for straightforward two-position automation. For their operation, it is necessary to supply a DC voltage to extend the actuator and reverse the polarity to retract it. The PQ12-R series micro linear servos operate as a direct replacement for standard rotary servos since they use the same three standard connectors [40]. These types of actuators have a maximum force of 50 N (see Table 8), which ensures that the payload below the gripper is lifted. The maximum stroke is 20 mm which allows adequate opening of the gripper to grab the payload. The gripper when closed has a base diameter of 90mm while once the fingers are extended, the usable diameter becomes about 120mm which is also the maximum diameter allowed for the payload.

The total weight of the system is 266 g. The value is obtained by summing the elements in Table 9 taking into account the number of elements required and in addition the mass of the 3 linear motors (see Table 8). The gripper extended height is 81 mm, while its

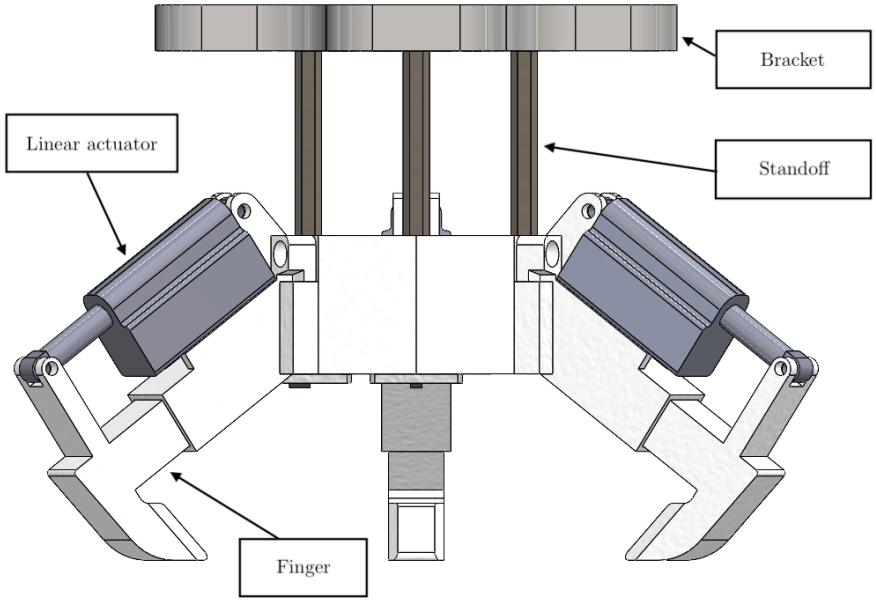

Figure 16: *First version of the gripper.*

Component	Mass[g]	Number of elements
Body center	72	1
Finger and case finger	16	3
Standoff	8	3
Bracket	52	1
Sensor housing	6	1

Table 9: *Mass properties.*

contracted height is 71 mm. This option was preferred for a second phase of testing since it increased implementation costs.

Second Version

In the second version of the gripper, it was chosen a different mode to move the finger in order to decrease the cost of the prototype. In this version, the fingers and finger holders of the first version were adapted to the new movement mechanism. However, the overall dimensions of the gripper remained about the same in terms of volume and weight. The actuation of each finger is based on a crank-rod mechanism (see Figure 17) that allows rotary motion to be transformed into linear motion. This mechanism consists of two

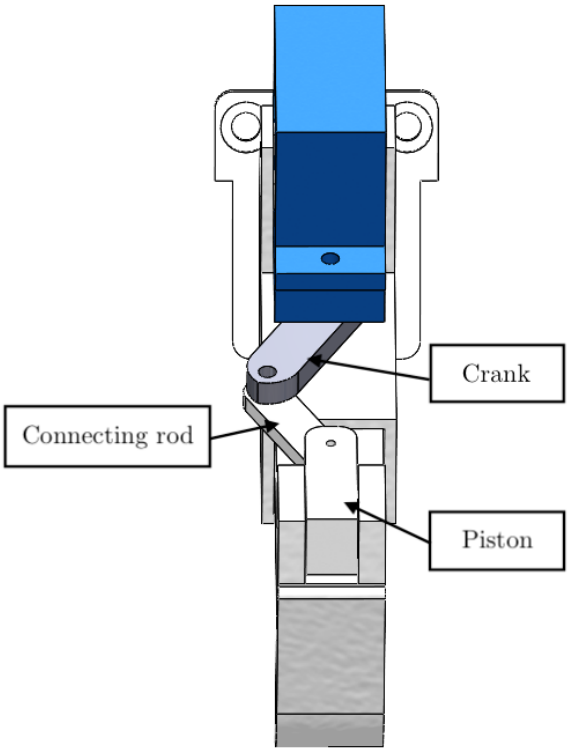

Figure 17: *Crank-rod mechanism.*

elements:

- Crank: it is the element of the connecting rod-handle mechanism that transforms the rotary motion of the shaft into the reciprocating motion of the plunger. An end crank is used that consists of a pin, called a "crank button," on which the connecting rod head articulates and is connected to the shaft by an "arm" [41].

- Connecting rod: it is the connection between the crank and the piston.

The lengths of the mechanism components were designed to achieve a 20 mm foot stroke so as to keep the same size as version one. The rotary motion is given by 3 servo motors FS90 from FEETECH. It is a 9 g analog servo that provides position control over an operating angle of 120° for standard servo pulses of between 900 ms and 2100 milliseconds duration. At 6 V, it has a maximum rotation speed of around 130 RPM

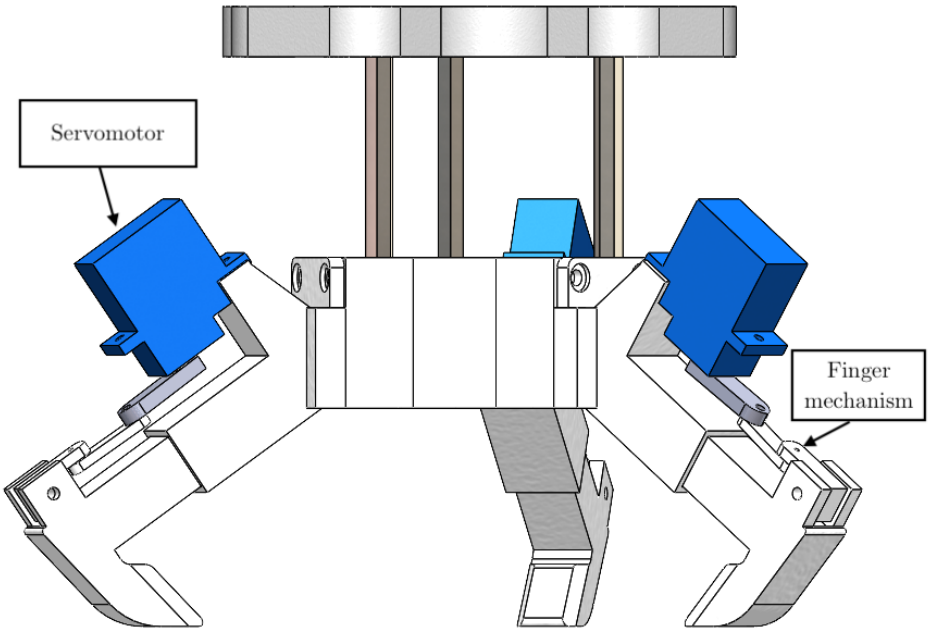

Figure 18: *Second version of the gripper.*

(no-load) and can produce up to 1.5 kg-cm of torque [42]. The servo is moved to the 0° position by a signal with a 1ms duration. The servo will be at the 90° position if the signal duration increases to 1.5ms. The servo will be at 180° from the starting position when the signal reaches 2 ms. The default rest point is 1.5 ms, but this can be changed by turning the middle-point positioner with a small slotted screwdriver. Pulse widths greater than the rest point cause counterclockwise rotation, with speed increasing as the pulse width decreases; pulse widths less than the rest point cause clockwise rotation, with speed increasing as the pulse width decreases.

4.2 Sensors

The compartment of sensors present is of two types so as to allow proper coupling between the gripper and the payload.

The sensors are:

Characteristics Phototransistor	
Dark current	50 nA
Half angle	12°
Collector current max	15 mA
Collector-emitter voltage max	35 V

Table 10: *Characteristics Phototransistor SFH 309 FA*

- A Matrix sensor that can be seen as a 25-pixels custom Charge-Coupled Device (CCD).
- Three Time of Flight sensors to improve and extend the measures of the matrix. These measure the distance to a target object by calculating the round trip time of photons, from the sensor to the object and back again [43]. TOFs are installed in the base of the central body of the gripper.

The matrix sensor is composed of two parts (shown in Figure 24):

- an infra-red LED, whose beam can be considered as a conic beacon and is attached to the payload;
- a 5x5 matrix of phototransistors, that is comparable to a 25-pixel custom CCD and is fixed in the center body of the gripper.

The reference axes are as drawn in Figure 19, in the x,y plane the phototransistor matrix is developed while the z-axis indicates the outgoing plane to the matrix. Osram SFH 309 FA Silicon NPN Phototransistors were used [44]. Its max collector current is 15 mA and the dark current is 50 nA (see Table 10). The half angle that it is the angle at which the light emitted by an LED is 50% or higher than its maximum intensity is equal to 12°. The operation principle of the matrix is based on the geometric fact that when a cone intersects a plane, it forms a different geometry that depends on the relative position and orientation of the cone vertex with respect to the plane. The plate is represented by the phototransistor array, and the cone, on the other hand, is represented by the main lobe of the infrared LED placed in the payload. Two main geometric shapes can be found as an image from the intersection of the two elements.

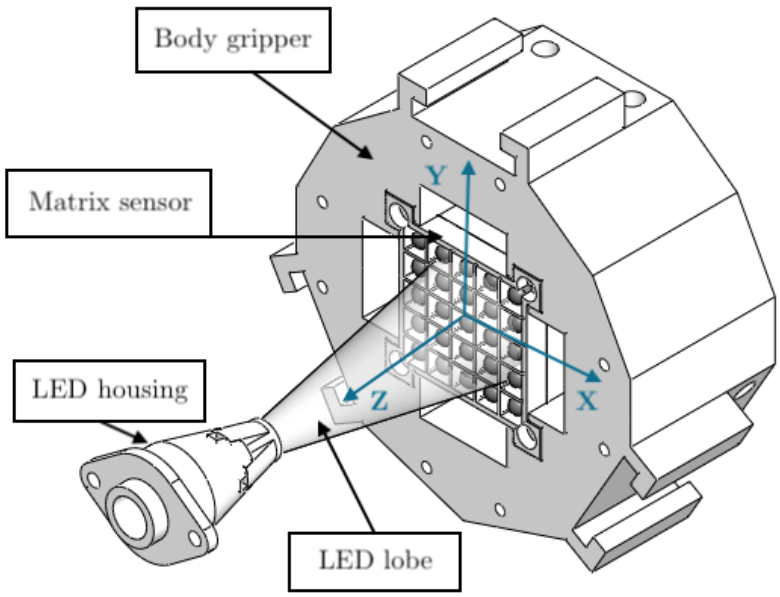

Figure 19: *Iteration between the cone formed by the LED and the phototransistor array.*

- CIRCLE: it is found when the base of the cone and the plate are parallel. The radius of the circle increases as the distance between the plane and the vertex increases.

- ELIPSE: it is found when the base of the cone and the plane are not parallel. The ellipse has a minor axis parallel to the axis of the relative rotation.

Tests were conducted to validate the operation of the system, especially to understand how the phototransistors lit up by changing the various distances. For this purpose, an experimental setup has been built. It is composed by placing the phototransistor array and the infra-red LED in two parallel planes, thus avoiding complex shapes as a result caused by tilting. The LED plane was mounted on a rail that allows it to slide along the z-axis while the phototransistor plane is fixed. A point was taken at each mm. The initial distance was 0 mm until it reached 100 mm, and for each step, the sensor saves the data for post-processing. For this project, 5 measures were reported to give an understanding of how the matrix works without going into too much detail. The chosen points are taken at a distance of 10 mm from each other starting from 0 mm and then reaching 40 mm (see Figure 21).

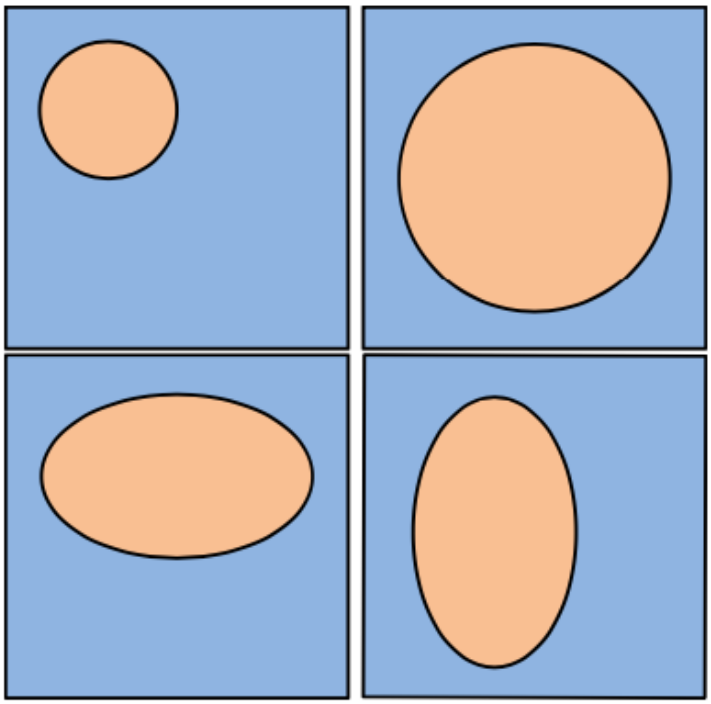

Figure 20: *Four different images project by a cone which intersects a plane. In the first two cases, the base of the cone and the plane are parallel, but the vertex is at two different distances.*

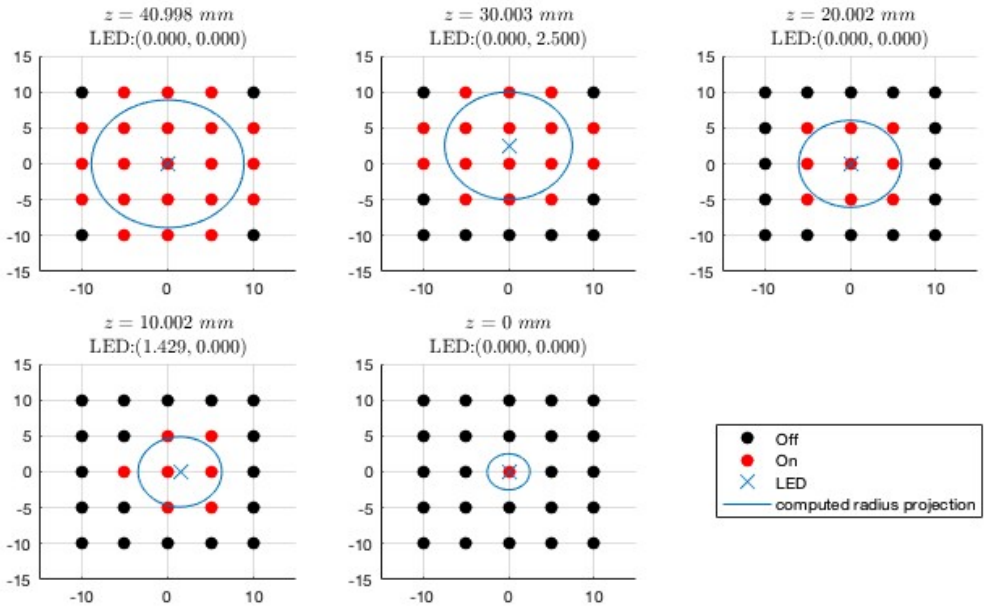

Figure 21: *Activation of the phototransistors with respect to the position of the gripper and LED in the z-direction*

At the 0 mm distance point, the only phototransistor lit is the center one while the

more the elements are moved (matrix, payload) the more the beam of lit phototransistors increases until 40 mm. At a distance of 40 mm, almost all phototransistors are illuminated. From this, it is understood that above 40 mm the accuracy of the sensor decreases significantly by no longer providing accurate information about its distance since the phototransistors are all illuminated. In addition to evaluating the slope of the cone vertex and the distance along z between the two elements, it is possible to evaluate the position in the x,y plane (see Figure 22).

The position in the plane is the distance between the barycenter of the projected image with the center of the reference system that corresponds to the central phototransistor. The resolution of this measurement is 5 mm, which corresponds to the distance between two phototransistors.

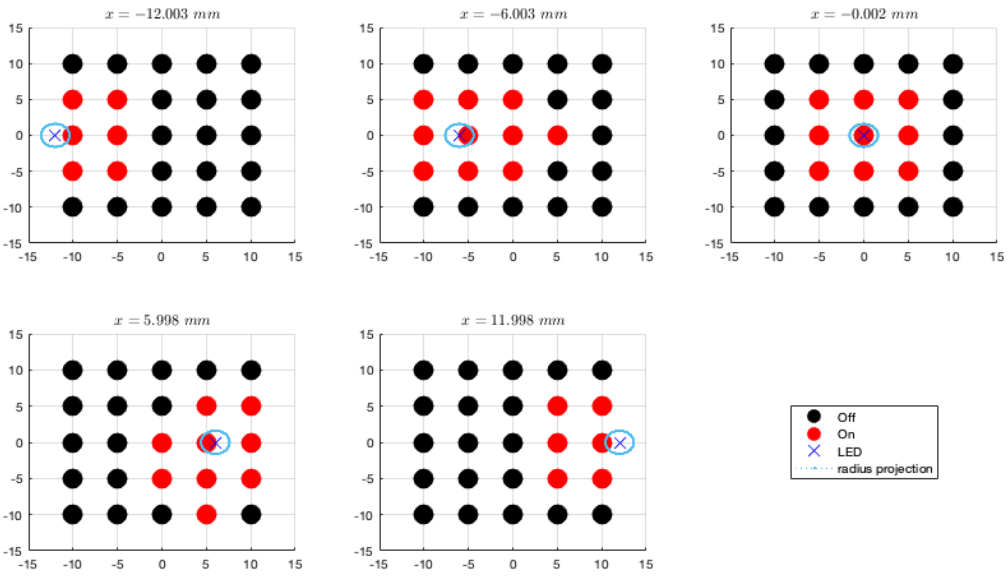

Figure 22: *Activation of the phototransistors with respect to the position of the gripper and LED in the x-direction*

In Figure 22, five distances were taken to show the projected images when moving the LED from left to right along the x-axis. With displacements greater than 15 mm, it can be seen that the phototransistors begin to stop detecting the underlying LED, and this is caused by the 12-degree half angle limiting the visual field. The sensors demonstrated

zero noise and thus high stability during these tests. This means that if the LED does not move, the projected image does not change. This property is due to the pull-up resistors that cause each phototransistor to behave as a digital device with a 0 or 1 output.

4.3 Electronic aspects

The gripper electronics are operated by a Raspberry Pi model 3B+ which is connected to two other boards in order to expand its capacity. These boards are:

- IoPi Plus AB Electronics that is used to expand the digital input. This board due to its 32 inputs is used to read the 25 phototransistors in the array. This board communicates with Raspberry through an I^2C (Inter-Integrated Circuit) communication which is a two-wire serial communication system used between integrated circuits.

- AdaFruit Motor Hat that is used to produce the PWM signals needed to drive the three finger motors. This board allows for reliability in the output signals, something that was lacking in the Raspberry. It communicates with Raspberry through an I^2C.

Figure 23 shows the developed circuit, including the pull-up resistors of each individual phototransistor. These resistors are used to properly bias digital port inputs, to prevent them from fluctuating randomly when there is no input condition thus obtaining a digital signal of 0 or 1.
The circuit also serves to group all of the feeding and ground lines, in addition to all of the lines for I^2C communication of the time of flight sensors.

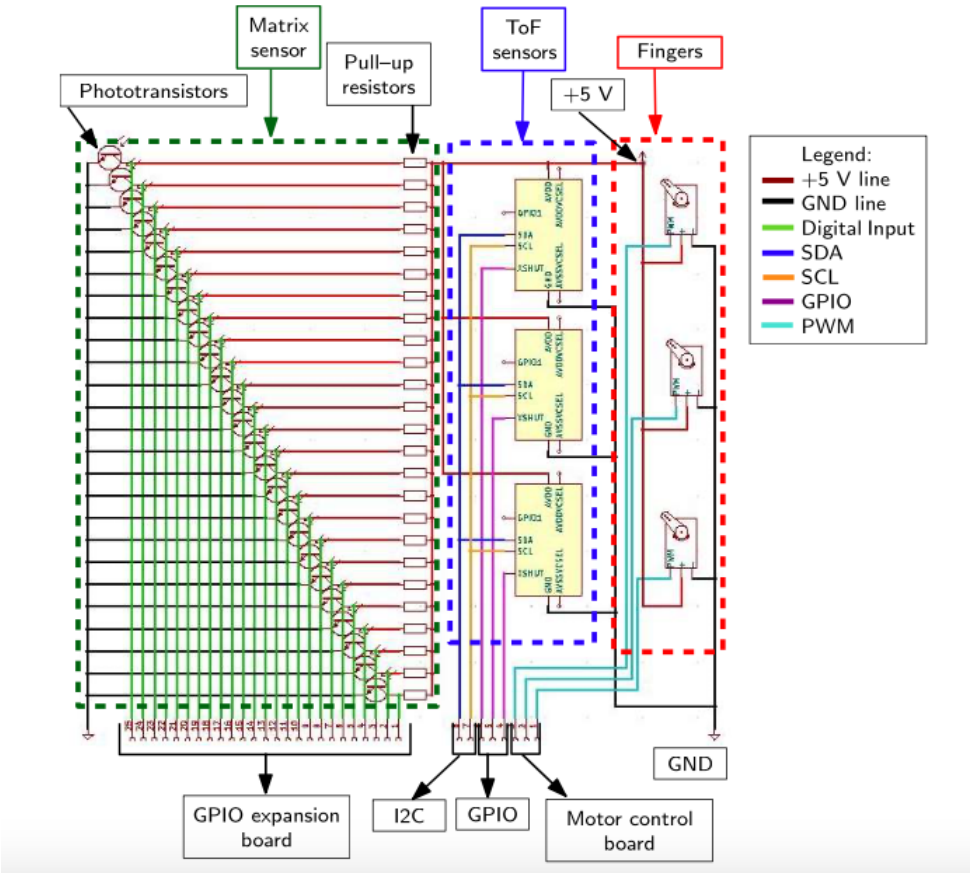

Figure 23: *The custom circuit to manage the electronics.*

4.4 Payload

The Payload was designed by incorporating the necessary devices for the docking mechanism. These devices are:

- Gripper interface is the part that comes in contact with the gripper. The circular design of the gripper interface permits the two elements to run smoothly without any problems of misalignment during the rotation. As a future option, there may be the inclusion of a second side matrix with its corresponding infrared LED in the payload, so that the rotation of the gripper can also be evaluated and adapted to the gripper interface.

- LED housing is used to hold the infrared LED in place inside. During acquisition, the matrix sensor must be in contact with the part above this piece so that only the

Characteristics SFH 4544	
Forward voltage(max)	1,6V (1,9V)
Reverse Voltage	5 V
Forward current	100 mA
Surge current	1 A
Half angle	10°

Table 11: *Technical characteristics of an infrared LED.*

central LED is displayed in the projected image. The infrared LED used is an SFH 4544 by OSRAM with a peak wavelength equal to 950 nm [45]. Other characteristics of the LED in Table 11.

- Battery is required to power the LED. The battery pack consists of 4 AAA batteries connected via a switch to the LED.

Four stand-offs were inserted under the gripper interface. In this way, the plate does not create obstruction problems during the docking phase. The weight of the payload is about 250 grams. The base is a square with a side dimension of 100 mm.

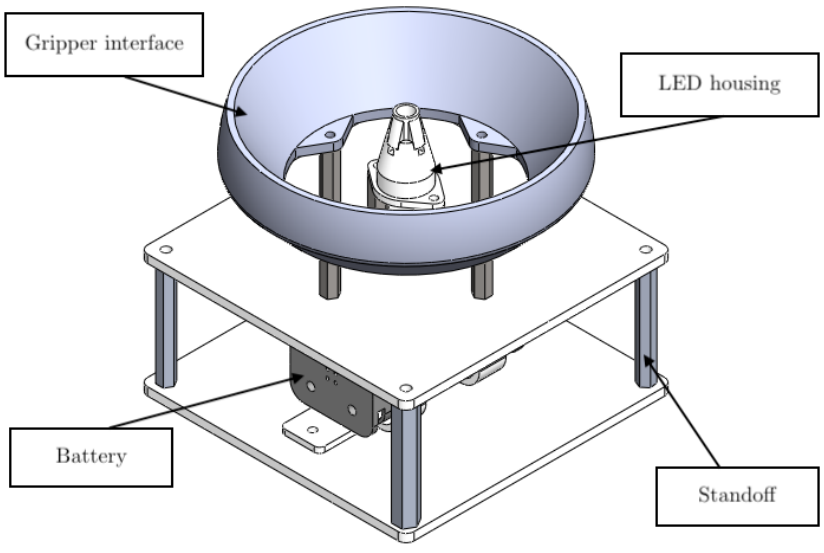

Figure 24: *The payload that includes the necessary sensors for the docking system and the clamp interface.*

5. Test

This chapter discusses the feasibility verification of the elements used for the docking system. The tests were chosen in increasing order of difficulty. It began with testing the various subsystems and components and progressed to testing the entire system. By using this method, it was possible to address all of the issues and challenges that arose during testing before moving on to more complicated systems. The testing campaign was divided into 4 main tests.

1. Test validation of gripper design.

2. Motor spin test.

3. Flight test.

4. Payload transport test.

5.1 Test validation of gripper design

The objective of this test was to validate the operation of the gripper design. The test was considered passed when the gripper was able to close, cling and hold up the payload and then open up again. This test is run to check for any components that could become stuck when the finger is moved. Additionally, it is used to estimate the tightness of servomotors

under load.

The equipment needed for the test is:

- Gripper.
- Payload.
- Arduino M0 PRO.
- Breadboard.
- Electrical cables.

The first step was to write the Arduino code to control the gripper servomotors. A time gap was inserted between the opening and closing phases of the gripper so that the operator could lift the payload and check the finger tightness. The code was uploaded onto Arduino M0 PRO with a USB cable. This board has an input voltage equal to 5-15 V, Power Consumption equals to 44 mA and it has 12 PWM output[46]. The servomotors have 3 cables: positive voltage, negative voltage and signal. Each motor was connected via the breadboard to the Arduino by choosing the pins highlighted in Figure 25. The setup for the first test was shown in Figure 16. During the test, the gripper was lifted manually to a height of 15 cm. The gripper passed the tests with difficulty after the initial stages of setting up the servo motors because some issues arose.

The problems that occurred in testing were:

1. **First problem**: Sliding between the finger and finger holder. This mechanism causes greater frictional forces between components since the initial rotation pushes the whole finger toward the finger case. The problem is also noticeable at the end of the finger stroke, which tends to get stuck. This problem is caused by suboptimal molding for some components that required smaller ABS filament sizes. This friction was limited by sanding the outer walls of the foot with different types of sandpaper and adding a generic mechanism grease.

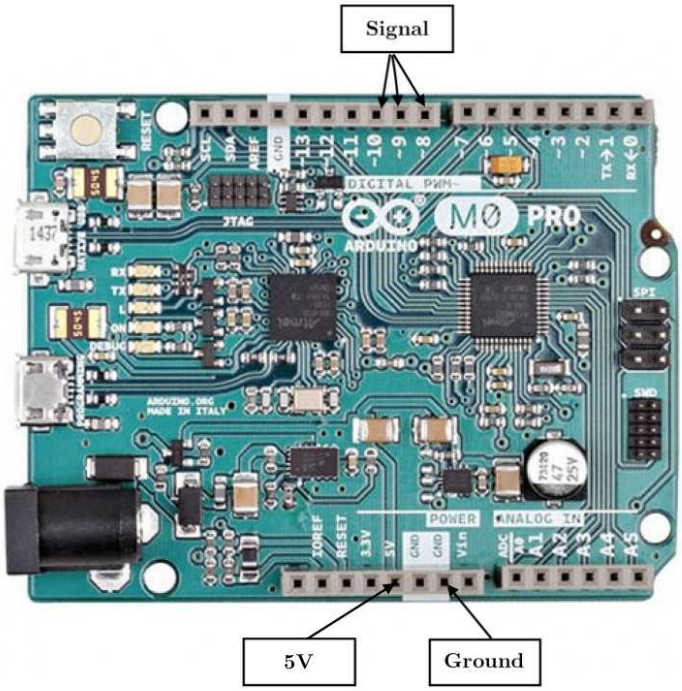

Figure 25: *Arduino M0 PRO.*

2. **Second problem**: Servomotors rotation. Due to the rotational motion of the servo, a holding screw was not sufficient to keep the element fixed. Rubber bands were used to try to avoid spinning. The bands allow the servo to move closer to the finger house and keep it on the same axis. By limiting these rotations, the thrust force was greater.

3. **Third problem**: Three pivots. There are three fulcrums in the configurations: one between the crank and connecting rod, the second between the connecting rod and piston, and the last to connect the piston on the finger. These fulcrums decrease the thrust force since there are many mechanical backlashes that occur in conjunction. Self-locking nuts and Teflon were used to improve this problem. Teflon was used to create friction between the screw and the nut and not allow loosening in the joint.

Once the assembly was verified to be working properly, the misalignment between the two parts was also tested. The misalignment between the centers of gravity cannot exceed 8-10 degrees. It was noted that the gripper can only capture the workpiece if the finger

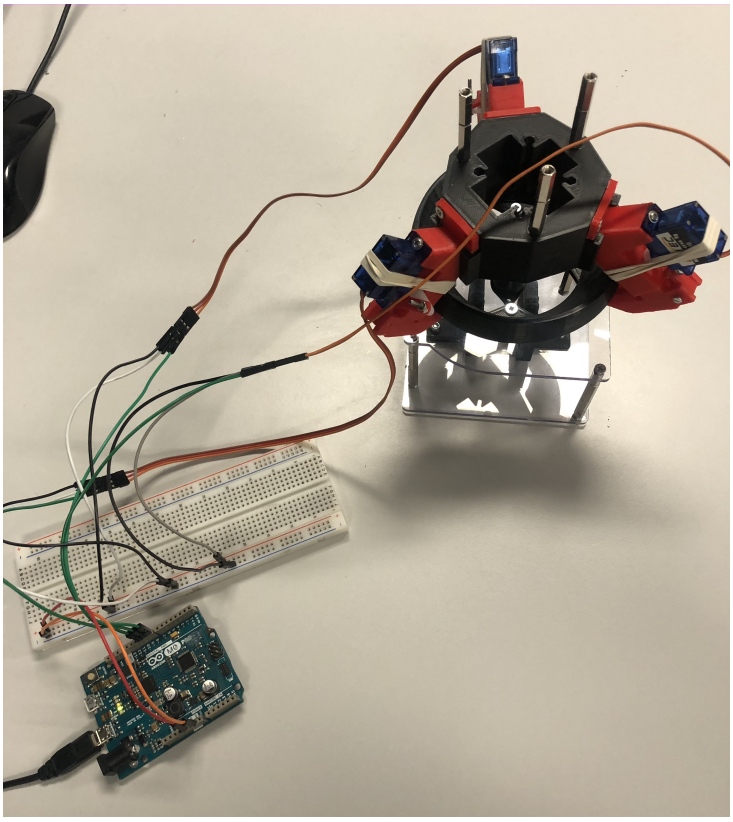

Figure 26: *Set up of the first test.*

can connect with the bevel in the payload interface. At greater angles, a finger would remain too distant to touch the interface below.

5.2 Motor spin test

The second test concerns the operation of the hardware needed to operate the drone alone. This test, therefore, aims to control the rotation of the drone motors. It was considered the motors because they are the terminal part of the connections. The components were assembled and attached to the frame, choosing the most appropriate arrangement to maintain the central center of gravity. Some items require preferred positions such as the flight controller, which must be centrally fixed according to a predetermined orientation, or the receiving antenna, which must have its receiving wires perpendicular. The motors receive the signal from the transmitter only once they are armed through the radio control. Before arming them, the safety switch must be pressed. The safety switch can be used to

enable/disable the outputs of motors and servos.

The equipment for the test is:

- Drone.
- Radio Transmitter (Futaba T8J).
- PC.
- USB cable.

The flight computer was connected to the PC through a USB cable. This link allows the user to see on the software the various error messages that could have occurred. The radio was used to arm the engines and increase their thrust. Once the battery was connected to the drone and the remote control was turned on, problems were noticed.

The GPS was the source of the initial issue. The GPS device needed data from at least 6 satellites in order to pass the pre-arm stage. Due to the poor coverage caused by the presence of buildings at the first test site, problems arose in connecting with the 6 satellites often losing the signal. It was feasible to verify that the GPS was operating properly at the second test location, which was in a park outside a city and away from signal-limiting obstacles. Once the GPS operation was tested, it was disabled from the pre-arm so that it could operate even in places with less than optimal satellite coverage. in this way, tests could be carried out in any useful and safe place even indoors. The GPS signal may be beneficial for some forms of navigation, but it has also been turned off to simplify all arming operations.

The second problem came from the signal input to the motors. The problem was not being sent via message to the software but only through an intermittent sound produced by the ESCs. The issue was caused by a low input PWM signal. The PWM signal can have a minimum value of 800 ms and a maximum value of 2200 ms. The minimum was set to 1100 ms because it had to be greater than the minimum of the receiver input. The receiver's minimum is 1075 ms. The minimum is chosen to be higher than the RC signal

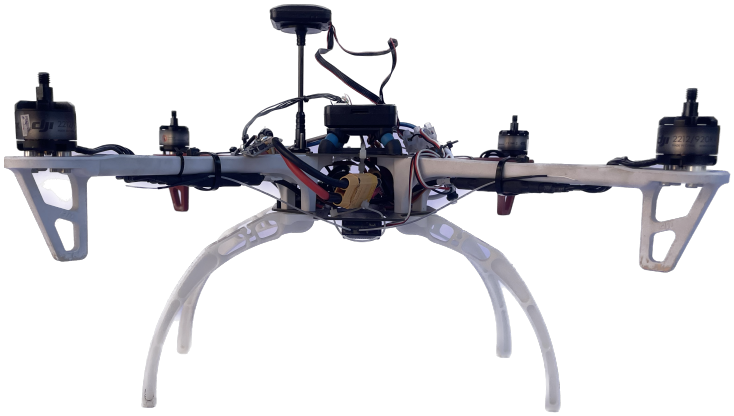

Figure 27: *First quadcopter drone prototype.*

in order to prevent the motors from being overpowered once the drone is armed. Too much power to the motors causes the drone to take off against the pilot's will. After the mistakes had been corrected, the motors spin had been determined. Since the drone must be steady, two must rotate clockwise, and two must rotate counterclockwise as specified in Section 3.1. This step is performed by the Mission planner, which allows the direction of rotation of the motor to be reversed. Through the software, it is also possible to start a single motor at a time to see if the rotation is as desired.

5.3 Flight Test

During the first test set-up phase, technical problems occurred with the motor power supply system, which led to a delay in the procurement of components. In order to obtain preliminary data on the docking system, however, it was decided to use a second prototype drone. The second quadcopter is also a prototype, but it is heavier and more powerful than the first. The drone has a tarot frame, and the propulsion system is made up of four DJI E600 sets. The single motor maximum thrust is 15 N/axis [47] so the maximum takeoff weight is approximately 6.5 kg. A 6-cell LiPo battery with a total voltage of 22.2 V is required for the system to function properly. In contrast to the first prototype flight computer, the DJI Naza M v2 regulates drone stability. Since it is a DJI component, specialized software that is no longer open source is required. For this phase,

a DJI 2.4 Ghz data link antenna with a BTU module was used to transmit drone data directly to the Ground Station. Ground Station is a DJI application that was used on an iPad and it's available in the App store. The antenna is powered by a USB port on the computer and sends data to the iPad. Through the app, it is possible to monitor the drone position, height and speed of movement. It is also possible to use the Ipad as a joystick to control the drone without using the radio control. This is possible when using the click-and-go flight mode.

The equipment for the test is:

- Drone.
- Radio Transmitter.
- PC.
- Ipad.
- DJI 2.4 Ghz data link antenna.

The objective of the test is to check the in-flight stability of the quadcopter and its ability to maintain itself in hover. The drone was flight tested in an open area to see how it responded to the pilot's commands and to see if the calibration performed by the software was correct.

The drone passed this test by completing the maneuvers given by the radio control without loss of signal. The initial calibration performed in the configuration phase was found to be in accordance with that desired so it allowed the drone to be stable as a neutral configuration. The GPS flight mode made it possible to maintain stability while hovering. This was made feasible by the 14 satellites that could be seen, which improve signal interpolation and lower measurement error. The drone can be programmed to follow a particular path thanks to the ground station. The path was divided into three phases: takeoff to 2 meters, move to the second point and landing above the payload. Because of the poor GPS accuracy, the actual landing distance to the payload on the ground

was nearly 1,50 m and varied depending on the satellites in view. In fact, it should be remembered that the GPS system has excellent but not absolute accuracy, equal under optimal conditions to 5 meters or even less and is affected by weather conditions and interference. This test demonstrated that without the use of sensors in the gripper, it is not possible to lock onto the payload using GPS coordinates alone.

A second change imposed after this test concerns the gripper. Since the drone is not very stable due to the wind and the movements are not as accurate as those of a robotic arm, it was decided to change the design of the gripper (see Figure 28). The new design allows for less friction between the parts and more finger travel without blocking at the end of the stroke. The central body remained the same as in previous versions. The finger stroke has increased from 20 mm to 25 mm thus allowing a greater margin of error in gripper-payload coupling. In this version, the arrangement of the propulsion mechanism components has changed. The servo has been shifted to the left by 12 mm so that it is misaligned with respect to the finger. The crank thrust is now found to be on the axis with the finger and the connecting rod. Also, a fulcrum was eliminated by connecting the connecting rod with the finger without going through an intermediate element. These elements were connected by an M3 screw. With axial thrust and one less fulcrum, the pressure losses are very limited compared with the initial configuration.

A solution was also found for the rotation of the servos so as to keep them as fixed as possible. A bracket was designed that wraps around the servo so it can be attached in two places. By wrapping the servo with the bracket, the lateral movement of the motor is almost totally limited. All the issues discovered in the initial test have been solved in this updated version, significantly enhancing the gripper behavior.

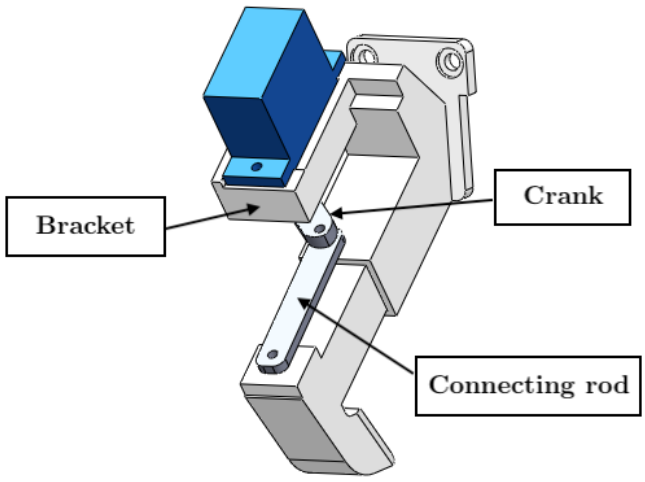

Figure 28: *Third gripper configuration. Designed on the improvements of the second version.*

5.4 Payload transport test

This test is performed to verify the feasibility of clinging a payload and moving it using only the drone with manual controls. The objective of this test is to move the payload between two established points by using the gripper to hook the payload at the first point and deposit it at the second point.

The equipment for the test is:

- Drone.
- Radio Transmitter.
- Payload.
- Two platforms.

The two takeoff and landing points were highlighted by placing wooden platforms so as to have as horizontal a base as possible. During the first trials, the drone during its landing accidentally hit the payload with its support feet. The payload then did not remain fixed in place but moved onto the platform. The payload was then inserted into a wooden frame,

Figure 29: *Payload positioning once docked.*

which locked the rotation in place. This was done to make engagement with the gripper easier. This test was completed, and a frame of the final video is shown in Figure 29. One of the problems that have hindered this test stems from the ground effect. This effect is affected by altering radically the aerodynamic field from that normally found when a flight is made at altitudes much greater than the diameter of the blades relative to any obstacle. When the quadcopter is close to the ground, vortex formation is hindered by the proximity of the ground and the induced drag decreases. This phenomenon promotes acceleration on takeoff while on landing it extends the trajectory, creating annoying turbulence. This turbulence decreased accuracy during landing. During the flight phase, the wind caused unintended displacements adjusted by corrections in the pilot's controls.

The gripper tightness was then tested by increasing the payload weight. For this test, several iron cubes with a total maximum weight of one kilogram were placed inside the payload structure. The iron cubes were chosen for immediate availability in the laboratory

and their high density since the free space within the payload is not high. The grapple showed no signs of failure and the finger-opening system has always worked smoothly. Given the greater power of the second prototype drone used, the greater weight of the payload did not affect the flight performance significantly.

6. Conclusions

The objective of this thesis was to validate and test the docking system developed for the AUTOMA project using a quadcopter drone in scenario C. This scenario attempts to deploy this technology on Mars and other worlds in addition to the terrestrial environment. The paper begins by outlining the current level of knowledge on drone use on Earth and prototypes created for interplanetary missions. The first unmanned aerial vehicle to land on Mars was Ingenuity. It demonstrated that flying to planets other than Earth is possible by overcoming atmospheric issues. It showed that it is possible to generate the lift required for flight even in a rarefied atmosphere. This UAV has allowed humans to start exploring distant planets not just on the ground with rovers but also in the air. There are considerable benefits since more distances may be traveled in a shorter amount of time in this fashion. It was feasible to construct the first prototype drone to test this docking technique thanks to thorough research on drones. It was then decided to test a quadcopter drone before optimizing the grapple to make it effective and feasible. Due to insufficient signal accuracy, cargo docking with GPS coordinates alone is not viable. This was shown in the autonomous flying test when an inaccuracy of a few meters was observed. The lack of sensitivity in the drone movements also caused difficulties in gripping the payload. This is due to the fact that the distance between the aperture of the gripper and the interface of the payload is only a few centimeters. Other sensors attached to the gripper are required to finish the verification of AUTOMA technology so that the operator has a

local reference as well as a distant one. Due to procurement delays, it was not possible to test the sensor package that was the subject of this thesis section 4.2. A significant technical advance in this environment would be achieved by using these sensors to perform autonomous docking on the cargo. This may open up a lot of doors for research and pave the way for completely autonomous driving. Consequently, a future of unmanned Martian exploration using autonomous platforms and vehicles is imaginable. It is obvious that this new exploration paradigm also applies to terrestrial scenarios, particularly those involving isolated locales with dangerous circumstances or harsh weather.

Bibliography

[1] S. P. Zdenek Ilich, Guillaume Grossir, O. Chazot, Review of the vki longshot hypersonic tunnel operation for martian entries, ResearchGate.

[2] Stabilità statica e dinamica di un multirotore, Available at `http://www.gizio.it/ENGLISH.htm`.

[3] Instruction manual futaba, Available at `https://futabausa.com/wp-content/uploads/2018/09/8J.pdf`.

[4] Simple overview of ardupilot operation, Available at `https://ardupilot.org/rover/docs/common-basic-operation.html`(2021).

[5] S. M. Christian Wankmüller, Maximilian Kunovjanek, Drones in emergency response – evidence from cross-border, multi-disciplinary usability tests, Elsevier.

[6] K. H. Kindervater, The emergence of lethal surveillance: Watching and killing in the history of drone technology, SAGE.

[7] S. M. S. . M. G. N. . F. R. . G. Izbirak1, Application of hierarchical facility location problem for optimization of a drone delivery system: a case study of amazon prime air in the city of san francisco, CrossMark.

[8] U. R. Mogili1*, B. B. V. L. Deepak, Review on application of drone systems in precision agriculture, Elsevier.

[9] B. E. Masoud Gheisari, Applications and requirements of unmanned aerial systems (uass) for construction safety, Elsevier.

[10] A. R.-v. W. Dylan Cawthorne, From healthdrone to frugaldrone: Value-sensitive design of a blood sample transportation drone, IEEE.

[11] How delivery drones are being used to tackle covid-19, Available at `https://blog.werobotics.org/2020/04/25/cargo-drones-covid-19/`.

[12] B. Mishraa, D. Garga, P. Narangb, V. Mishraa, Drone-surveillance for search and rescue in natural disaster, Elsevier.

[13] T. Zweglinski, The use of drones in disaster aerial needs reconnaissance and damage assessment – three-dimensional modeling and orthophoto map study, MDPI.

[14] S. H. A. Aris A. Almalki, Ben Othman Soufiene, H. Sakli, A low-cost platform for environmental smart farming monitoring system based on iot and uavs, MDPI.

[15] A. Bouskela, A. Chandra, J. Thangavelautham, S. Shkarayev, Attitude control of an inflatable sailplane for mars exploration, Arxiv.

[16] E. Petritoli, F. Leccese, Unmanned autogyro for mars exploration: A preliminary study, MDPI.

[17] M. R. Jardin1, R. Shenoy2, Introducing the model-based aerospace challenge (mach), ResearchGate.

[18] NASA, A concept study of a remotely piloted vehicle for mars exploration, NASA.

[19] G. C. Birur, K. R. Johnson, K. S. Novak, T. W. Sur, Thermal control of mars lander and rover batteries and electronics using loop heat pipe and phase change material thermal storage technologies, NASA.

[20] G. L. Anthony Colozza, V. Lyons, Overview of innovative aircraft power and propulsion systems and their applications for planetary exploration, NASA.

[21] NASA, Mini-sniffer.

[22] C. A. Kuhl, Design of a mars airplane propulsion system for the aerial regional-scale environmental survey (ares) mission concept, NASA.

[23] M. P. G. J. Balaram, MiMi Aung, The ingenuity helicopter on the perseverance rover, Springer Nature.

[24] Mage, Available at `https://www.msss.com/news/index.php?id=11`.

[25] Venus atmosphere, Available at `http://www.ajax.ehu.es/VEX/Venus.Earth/Venus.Earth.html`.

[26] G.AcostaM.Hassanalian, Power minimization of fixed-wing drones for venus exploration in various altitudes, Elsevier.

[27] A. A. M. Hassanalian, D. Rice, Evolution of space drones for planetary exploration: A review, Elsevier.

[28] Space debris, Available at `https://www.nasa.gov/mission_pages/station/news/orbital_debris.html`.

[29] Darpa's phoenix program, Available at `https://www.darpa.mil/news-events/2014-04-02`(2014).

[30] T. J. Walter Mirczak, Satlets - the building blocks of future satellites - and which mold do you use ?, ResearchGate.

[31] N. T. Redd, Bringing satellites back from the dead: Mission extension vehicles give defunct spacecraft a new lease on life, IEEE.

[32] Osam-1 mission on-orbit servicing, assembly, and manufacturing 1, Available at `https://nexis.gsfc.nasa.gov/OSAM-1.html`.

[33] Mars helicopter/ingenuity, Available at `https://mars.nasa.gov/files/mars2020/MarsHelicopterIngenuity_FactSheet.pdf`.

[34] A. Basit, M. Awais, M. Ullah, S. U. A. Shah, Design and fabrication of a quadcopter delivery drone, ResearchGate.

[35] Px4 flight controller, Available at https://docs.px4.io/v1.9.0/en/flight_controller/pixhawk.html(2020).

[36] E300 user manual v1.00, Available at http://dl.djicdn.com/downloads/tuned-propulsion-system/e300/en/E300_User_Manual_v1.00_en.pdf(2013).

[37] Reliable electric drive simulations, Available at https://www.ecalc.ch/xcoptercalc.php(2022).

[38] Ardupilot, Available at https://ardupilot.org/.

[39] A. Caon, Development of a smart capture system for on-orbit servicing with space robots.

[40] Pq12-r actuonix, Available at https://www.actuonix.com/pq12-r.

[41] Dimensionamento della manovella di un meccanismo biella-manovella, Available at http://www.edu.lascuola.it/edizioni-digitali/NuovoPrincipiMeccanica/Manovella.pdf.

[42] Feetech fs90r micro continuous rotation servo, Available at https://www.tme.eu/Document/466f036ded06bd5cfbf8271c3502f528/POLOLU-2820.pdf.

[43] Nozioni fondamentali sulla misurazione della distanza e sul riconoscimento dei gesti mediante sensori tof ., Available at https://www.digikey.it/it/articles/fundamentals-distance-measurement-gesture-recognition-tof-sensors.

[44] Osram sfh 309 fa, Available at https://www.osram.com/ecat/Radial%20T1%20SFH%20309%20FA/com/en/class_pim_web_catalog_103489/prd_pim_device_2219658/.

[45] Osram sfh 4544, Available at https://www.osram.com/ecat/Radial%20T1%203-4%20SFH%204544/com/en/class_pim_web_catalog_103489/prd_pim_device_2219771/.

[46] Arduino m0 pro., Available at https://docs.arduino.cc/retired/boards/arduino-m0-pro.

[47] Dji e600, Available at https://www-v1.dji.com/product/e600/spec.html.